WORKING paper

BANQUE DE FRANCE
EUROSYSTÈME

Decomposing the Inflation Response to Weather-Related Disasters[1]

Erwan Gautier, Christoph Grosse-Steffen, Magali Marx & Paul Vertier[2]

December 2023, WP #935
(updated May 2024)

ABSTRACT

This paper provides a novel instrumental variable approach for the estimation of dynamic causal effects of weather-related disasters on consumer prices. We compute compositional effects by combining monthly granular inflation rates for 12 CPI product categories with weights in consumption baskets from French overseas territories. We find that disasters lead to a maximum rise in consumer prices of 0.5% with substantial heterogeneity in the price response. An immediate strong surge in the prices of food, and notably of fresh products, is partially offset by a decline in the prices of manufactured products and services. The effects of weather-related natural disasters dissipate after four months and differ along the income distribution, notably raising inflation more for low-income households. Evaluating a policy that implemented price caps in 2013, we find that price regulation dampened the price response on impact, but did not prevent prices from adjusting in the long run.

Keywords: Natural Disasters; Extreme Weather; Inflation; Disaggregate Inflation; Inequality; Price Gouging

JEL classification: E31, Q54

[1] We would like to thank Eric Strobl for an excellent discussion, and seminar participants at Toulouse School of Economics, University of Marseille, EEA-ESEM Congress 2023, T2M Conference 2023, Banque de France and IEDOM (Institut d'Emission des Départements d'Outre-Mer) for useful comments and suggestions.The views expressed in this paper are those of the authors and do not necessarily represent those of the Banque de France or the Eurosystem.

[2] Banque de France, erwan.gautier@banque-france.fr, christoph.grossesteffen@banque-france.fr, magali.marx@banque-france.fr, paul.vertier@banque-france.fr.

NON-TECHNICAL SUMMARY

How do weather-related disasters affect consumer prices? At a time when central banks are considering climate risks in their operational frameworks, this question is becoming relevant for monetary policy. Existing empirical literature has mainly focused on the overall effect on prices, cloaking the complex interplay of supply disruptions following natural disasters that drive up prices in the short run, combined with a shock to the composition of aggregate demand. This paper documents how prices of granular Consumer Price Index (CPI) product categories respond to weather-related natural disasters. The full decomposition across product categories in geographically small regions refines our understanding of the inflation response to extreme weather events. Given that disasters are expected to become more frequent as a result of climate change, our findings help policymakers to address the important challenge posed by uncertain climate change more appropriately.

A challenge for the measurement of causal dynamic effects from weather-related disasters is the imprecise measurement of economic damages resulting from asset impairment and business interruptions following natural disasters, which are not directly observable. We propose an empirical strategy that combines events from two disaster databases and different meteorological records to assess the intensity of economic damage in a first-stage regression, which can account for various country-specific factors that determine the relationship between the intensity of weather events and economic damages at the local level. By doing so, we select economic disasters that we can directly connect to extreme meteorological events. To assess the inflation effects of natural disasters, we then relate the economic disasters as predicted by the first-step equation to the evolution of prices for different time horizons following the shock. We focus our empirical analysis on prices in four French overseas territories, namely Guadeloupe, Martinique, French Guiana and Réunion.

Figure: Decomposition of the reaction of total inflation to a weather-related disaster

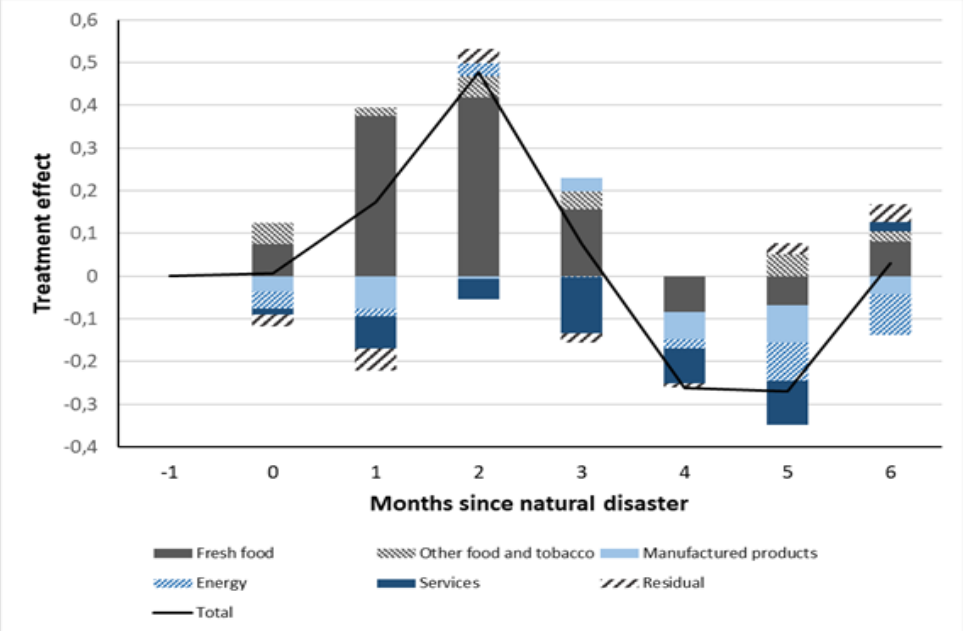

Note: Decomposition of the cumulative impulse response of headline CPI to a natural disaster in the baseline specification. The contribution of each component is computed as the cumulative response of the CPI of this component times its average weight in the consumer baskets of the four DCOMs between 1999 and 2018. Treatment effects are expressed in percent.

We find that weather-related disasters induce a temporary but statistically significant rise in headline consumer prices, with a peak at 0.5 percent two months after the disaster occurrence (Figure). The overall observed effect is driven by an immediate strong surge in the prices of fresh food products of 11 % after two months, which vanishes after four months. Prices of other food products also increase, but more moderately and in a more sustained manner (+0.3 %). By contrast, the prices of services and manufactured products decline moderately (and in a less statistically significant way), by about -0.2 %. The positive effects on food prices are likely to reflect negative supply shocks, as we observe a simultaneous decrease in agricultural employment. To the contrary, the negative effects on the prices of manufactured products and services are likely to reflect negative demand shocks.Our results point to small and temporary effects on headline inflation, mainly related to distortions of relative prices.

These effects translate into distributional effects through the heterogeneity in household consumption structure. Overall, the weather-related disasters increase temporarily inflation inequality, with a difference of up to 0.2 pp between the bottom and upper quintiles of the household income distribution. The rise in inflation inequality is primarily due to the fact that the weight of food in the consumption basket is higher for low income households.We also analyse the effects of the introduction of price cap policies, namely the *Bouclier Qualité-Prix* introduced in 2013. Price caps lower the impact response of price reactions to weather-related disasters in the sample period. However, cumulated over six months, price reactions are not significantly affected by the introduction of price cap policies, implying that the adjustment in the price level is just spread over the horizon of six months.

Décomposition de la réponse de l'inflation aux catastrophes météorologiques

RÉSUMÉ

Cet article propose une nouvelle approche par variable instrumentale pour estimer de façon causale les effets dynamiques des catastrophes météorologiques sur les prix à la consommation. Nous estimons des effets de composition en combinant les taux d'inflation mensuels granulaires de 12 catégories de produits de l'IPC avec leurs pondérations dans les paniers de consommation des départements français d'outre-mer. Nous constatons que les catastrophes entraînent une hausse maximale des prix à la consommation de 0,5 %, avec une forte hétérogénéité dans la réaction des prix. Une forte hausse immédiate des prix des denrées alimentaires, et notamment des produits frais, est partiellement compensée par une baisse des prix des produits manufacturés et des services. Les effets des catastrophes naturelles liées aux conditions météorologiques se dissipent après quatre mois et diffèrent selon la distribution des revenus, augmentant notamment davantage l'inflation pour les ménages à faible revenu. En évaluant une politique qui a mis en œuvre des plafonds de prix en 2013, nous constatons que la réglementation des prix a atténué la réaction des prix à l'impact, mais n'a pas empêché les prix de s'ajuster à long terme.

Mots-clés : catastrophes naturelles ; conditions météorologiques extrêmes ; inflation ; inflation désagrégée ; inégalité ; gonflement des prix

1. Introduction

How do natural disasters affect consumer prices? At a time when central banks are considering climate risks in their operational frameworks, this question is becoming relevant for monetary policy (e.g. Schnabel, 2021). Existing empirical literature has mainly focused on the overall effect on prices, cloaking the complex interplay of supply disruptions following natural disasters that drive up prices in the short run, combined with a shock to the composition of aggregate demand. This paper documents how prices of granular Consumer Price Index (CPI) product categories respond to weather-related natural disasters. The full decomposition across product categories in geographically small regions refines our understanding of the inflation response to extreme weather events. Given that disasters are expected to become more frequent as a result of climate change, our findings help policymakers to address the important challenge posed by uncertain climate change more appropriately (Hansen 2022).

We identify causal dynamic effects from weather-related natural disasters in an instrumental variable (IV) approach. To our knowledge, this paper is the first one to propose an IV setup for this type of question. A challenge in this field is the imprecise measurement of economic damages resulting from asset impairment and business interruptions following natural disasters, which are not directly observable. The existing empirical literature solves this issue by referring to one of two main approaches. The first approach constructs shock variables directly from administrative databases that detect an event based on *ad hoc* criteria, sometimes complemented by reporting-based intensity measures e.g. from insurance companies. Administrative databases have the advantage of identifying disasters with significant economic damage with a relatively high accuracy. However, they are also known to be subject to various reporting biases, which question the assumption of exogeneity of the disaster variable with regard to the endogenous outcome. The second approach uses only arguably *objective* meteorological and geophysical data in order to approximate the severity of the disaster event by the physical intensity, usually expressed in the quantity of precipitation, wind speed or the earthquake Richter scale. Meteorological and geophysical data predict hazardous incidents imperfectly, as events of similar physical amplitude are associated with different levels of destruction depending on regional vulnerabilities.[1] Therefore,

[1] The extent of economic damage is affected by geological features such as the degree of urbanization and land use in the affected area (Noy, 2009), or the shape of the continental shelf and coast (Bertinelli and Strobl, 2013). Further, damage from an incident of similar geophysical strengths can be dampened through adaptation measures, which themselves are a function of a number of determinants such as the ex-ante exposure to risks (Schumacher and Strobl 2011), the quality of institutions (Kahn 2005), and economic development (Felbermayer and Gröschl 2014).

researchers need to devote great care in directly modeling the underlying relationship in damage functions.[2] Damage functions, however, may be prone to specification errors since they are sensitive to thresholds above which e.g. wind and rain generate physical damage. Appropriate calibration values might not always be readily available. In a context in which countries adapt to the consequences of climate change, the relationship between meteorological records and economic damages are likely to differ not only across regions, but also over time.

To overcome these challenges for identification, we propose an IV strategy in a two-stage regression approach. To this end, we combine events reported in the international disaster database (EM-DAT) with a French administrative data set that collects information on natural disasters at the municipal level. We then use different meteorological records as instruments for the intensity of economic damage in a first-stage regression, which can account for various country-specific factors that determine the relationship between the intensity of weather events and economic damages at the local level. By doing so, we select economic disasters that we can directly connect to extreme meteorological events. To assess the inflation effects of natural disasters, we then relate the economic disasters as predicted by the first-step equation to the evolution of prices for different time horizons following the shock using a local projection method *à la* Jordà (2005). We are thus able to derive the causal dynamic price response both at the product level for different product categories and at the aggregate level following a given natural disaster shock (Stock and Watson 2018).

We focus our empirical analysis on prices in four French overseas territories, namely Guadeloupe, Martinique, French Guiana and Réunion. These regions are regularly exposed to significant weather-related disasters and are located in different parts of the world, which allows the study of shocks that are de-synchronized across regions. For each of these regions, we use highly harmonized price indices produced by the French statistical office (INSEE), at a disaggregate product level and available at a monthly frequency over the 1999-2018 period. There is a trade-off when considering the optimal size of regions for this type of analysis. While large regions contain the risk that the shock only imperfectly propagates to the economic outcome variable, small regions might limit the generalizability of the findings regarding the channels of shock propagation. While the regions considered here are rather small and isolated, they are comparable to a laboratory experiment that allows identifying precisely the effects of extreme weather events on prices by

[2] See for applications Emanuel (2011) and Strobl (2011, 2012), and for methodological review articles Auffhammer (2018) and Kolstad and Moore (2020).

matching information on natural disasters and product-level price indices for each of the four regions.

Our main results are as follows. First, we find that weather-related disasters induce a temporary but statistically significant rise in headline consumer prices, with a peak at 0.5% two months after the disaster's occurrence. The overall observed effect is driven by an immediate strong surge in the prices of fresh food products of 11% after two months, which vanishes after four months. Prices of other food products also increase, but more moderately and in a more sustained manner (+0.3%). This positive inflation effect coincides with a negative impact from natural disasters on agricultural employment, pointing to a negative supply shock with a displacement of labor supply from the agricultural sector to other low-skilled occupations as also found by Kirchberger (2017). Our findings on food products are consistent with the response of retail prices following typhoons in China. Bao, Sun and Li (2022) document that fresh products drive the overall response in food prices. By contrast, the prices of services and manufactured products decline moderately (and in a less statistically significant way), by about -0.2%. Overall, our results point to small and temporary effects on headline inflation, mainly related to distortions of relative prices.

Second, we quantify distributional consequences from natural disasters across income groups. We measure household-specific consumption structure for different income groups relying on household survey data. Using these weights by income group, the product-level price responses to natural disasters are aggregated to obtain heterogeneous price responses by income group (Hobijn and Lagakos, 2005, Hobijn et al., 2009). Since the effect on fresh food prices is positive and much stronger than any other product category, the effect on total inflation strongly depends on the share of fresh food in the consumption basket. We find that the upward effect on headline prices after two months is of 0.6% in the bottom quintile of the income distribution, i.e. 0.1 pp above the average effect. The upper quintile, in contrast, experiences a rise in consumer prices of 0.4%, i.e. 0.1 pp below the average effect. Overall, natural disasters have a positive effect on inflation inequality across income groups, but this impact is only transitory.

Third, we investigate the effectiveness of price cap policies. Specifically, we document that after the implementation of a price cap on a set of first necessity goods in 2013 (*Bouclier Qualité-Prix,* BQP), the increase in fresh product prices following a natural disaster was much smaller in magnitude. The stronger reaction of prices before the BQP points towards the existence of price gouging in the absence of regulation. However, consistent with a large literature we find that price gouging is unlikely to explain all of the observed effect. Indeed, after six months, the cumulated price response before and after the introduction of price caps are or similar magnitude, as price

increases after the BQP are more persistent, suggesting that even in the presence of price-cap regulation, retailers increase their prices after a natural disaster but in a more staggered way.[3]

Our main contribution to the existing literature is twofold. First, this paper shows that a rather small aggregate effects of weather-related natural disasters on headline inflation are the result of quite heterogeneous and partly off-setting price responses across product categories, which have not been documented at this level of granularity before. Parker (2018) and Kabundi et al. (2022) use data from the EM-DAT international disaster database and relate these events to CPI inflation in a large cross-section of countries. These two studies find strong heterogeneity in the impact of disasters on inflation across disaster types and the country development level. They also both emphasize the specific effect of natural disasters on food price inflation. Heinen et al. (2018) estimate the impact of hurricanes and floods on prices in Caribbean islands via calibrated damage functions. They inspect total headline CPI and three sub-categories, namely food, housing and utilities, and all other items. Their baseline result is an inflationary effect from disasters, lasting one month in response to floods and two months in response to storms. In line with our findings, food price is the sub-component that reacts most strongly to disasters. However, no offsetting effects are found in product sub-categories, possibly due to the still high level of aggregation of the "other goods" category. Our contribution is the estimation of the price response to natural disasters for a fully exhaustive list of product categories of CPI inflation that covers 12 types of goods and services. A highly balanced panel allows us to interpret our findings as compositional effects of headline inflation with larger granularity. A focus on a homogenous set of relatively small territories frequently exposed to extreme weather events allows us to estimate dynamic causal effects at monthly frequency with high precision. Finally, integrating sectoral economic dynamics enables us to discuss plausible narratives for shifts in sectoral supply and demand.

Our second contribution consists of proposing an IV approach for the estimation of causal dynamic effects of natural disasters. Specifically, the IV approach addresses the concern of reporting biases in administrative databases, which are likely to generate both attenuation biases (Grislain-Letremy, 2018) and sampling biases (Felbermayer and Gröschl, 2014). In a comparison across methodologies, we find that using administrative data only in a simple ordinary least squares (OLS) framework tends to underestimate the price effects of extreme weather events compared to the baseline specification. When comparing our results with those obtained from a calibrated damage

[3] See also the large literature on price gouging during crises, which generally finds limited effects (Cabral and Xu, 2021, Beatty et al., 2021, Gagnon and López -Salido, 2020; Neilson, 2009; Culpepper and Block, 2008).

function, our baseline results are broadly consistent, while the point estimate from a damage function approach remains below the effects found in the IV setting.

In this context, we highlight the careful modeling of regional seasonality. Most empirical contributions that evaluate the impact of natural disasters on inflation control for average time-specific fixed effects. This modeling approach ignores the fact that the seasonality of extreme weather events usually varies across territories and thus, is likely correlated with seasonality of inflation. This is in particular a concern for products locally produced. In order to account for this possible source for omitted variable bias, we include region-specific monthly dummies on top of month-year fixed effects. This modeling of seasonality further insures instrument exogeneity. Quantitative results change significantly if the model does not account for such regional seasonality.

Finally, the paper relates to the literature studying the consequences of natural disasters for inflation dynamics. Cavallo et al. (2014) and Doyle and Noy (2015) analyze the reaction of prices to large earthquakes in the form of event studies. Parker (2018) and Kabundi et al. (2022) use a variety of natural disasters, ranging from geophysical events to extreme weather events, distinguishing the intensive margin of disaster-types on prices. A few papers study weather-related disasters only, as we do. One specific strand of papers focuses on temperature variations (Faccia et al., 2021, Ciccarelli et al., 2023, Kotz et al., 2024).

The paper is structured as follows. Section 2 describes the data. Section 3 lays out the empirical strategy. Section 4 contains the main results. Section 5 presents distributional effects and implications from a price cap policy. Section 6 provides robustness checks, and section 7 concludes.

2. Data on inflation and weather-related disasters in French overseas territories

In this section, we describe how we combine detailed information on natural disasters and prices for French overseas territories, for the period from January 1999 to April 2018.

2.1 Product-level inflation data

We use the Consumer Price Index (CPI) produced monthly by INSEE for each of the four oversea territories, which we refer to as DROMs (*départements et régions d'outre-mer*). In France, there is no regional price index available. French overseas territories are the only subnational regions for which price indices are specifically calculated using price quotes collected in each region. These consumer price indices have been computed since 1967 in Guadeloupe, Martinique and Réunion,

and since 1969 in French Guiana. The methodology used for their computation is similar to that of the metropolitan CPI since 1993 and has been incorporated into the CPI for France since 1998. Price indices are published monthly at a granular level for 12 CPI components, along with their annual weight in the consumption basket. Table A.1 in the Appendix displays the summary statistics of price indices used.

There are some specificities of consumer prices in overseas regions, where prices are set in a distinctive manner compared with metropolitan France. First, price levels are generally higher in overseas regions, notably because of food prices, and the price gap remained broadly constant between 1985 and 2010 (Berthier et al., 2010). Second, as documented in Table A.2 in the Appendix, even though inflation in overseas regions is significantly correlated with inflation in metropolitan France,[4] the correlation is lower for food inflation (Hugounenq and Chauvin 2006), and especially for fresh products.

Second, the heterogeneous correlation of CPIs between metropolitan France and overseas regions is likely to reflect heterogeneous trade prevalence across types of goods and services. Indeed, according to Hugounenq and Chauvin (2006) about 45% of DROMs' final household consumption was imported in 1999 (of which 60% came from metropolitan France). The share of imported goods was as high as 70% for manufactured products and 90% for durables and fuels. In stark contrast, the food sector depends much more on local production. In 1995, between 55% and 63% of food needs were covered by local products. In general, coverage ratios are higher for fresh products than for "all food" products (combining fresh and processed foods), reflecting a higher prevalence of imports for processed foods.[5]

Third, French overseas regions benefit from specific fiscal schemes to compensate for their distance from metropolitan France: VAT is lower and a specific tax on imported products, protects local production against external competition (*octroi de mer*). Tobacco and petroleum products are also taxed differentially in the DROMs and in metropolitan France: no VAT is

[4] Several factors can explain this positive correlation. First, the consumption structure of overseas regions converged progressively with that of metropolitan France (with a decrease in food consumption and an increase in services consumption), partly reflecting a catch-up policy linked to the *départementalisation* of these four territories (i.e. their transformation into French *départements* starting in 1946). Second, price-setting mechanisms are to a large extent jointly determined between overseas regions and metropolitan France: the minimum wage in overseas regions has been aligned with that of metropolitan France since 1996, public compensations are identical (albeit with a premium compensating for the distance from metropolitan France), as are quality norms and rent-setting mechanisms.

[5] Table A.3 in Appendix A reports coverage ratios based on data from the *Observatoire des économies agricoles ultramarines*.

imposed on petroleum products, and taxes on tobacco are decided by local authorities. Furthermore, petroleum product prices are set by local authorities.

2.2 Weather-related disaster data

This section presents the data sources for natural disasters and extreme weather events.

2.2.1 Administrative databases for natural disasters

In this paper, we use two different data sets that collate administrative information on economic losses due to natural events.

First, we use the French administrative data set GASPAR (*Gestion Assistée des Procédures Administratives relatives aux Risques*) that collects information on the assisted management of risk-related administrative procedures and that is assembled by the French Ministry of Ecological Transition. This data set lists all natural disasters by municipality since 1990. In it, a disaster is recorded upon declaration by the French government of a state of "natural disaster", after consultation by an inter-ministerial commission. Importantly, the declaration of state of natural disaster conditions the eligibility of households to an insurance compensation. The GASPAR data set contains various information, such as the starting date and the ending date of the event, the code of the municipality, the location, and the designation of the risk. In this setting, we identify events that include designations of floods, tropical storms or cyclones as natural disasters.[6] By aggregating daily information, we build a monthly indicator variable per region. In the empirical analysis, we consider that the month of the natural disaster corresponds to the date when the disaster began.

We complement this data with information coming from the EM-DAT international disaster database, produced by the Centre for Research on the Epidemiology of Disasters (CRED) with a global coverage. The events recorded in the database are aggregated from several sources, namely insurance companies, UN agencies, NGOs, research institutes and press agencies. Events recorded in EM-DAT must respect at least one of three criteria: (i) 10 or more people killed; (ii) 100 or more people affected/injured/homeless; and (iii) declaration by the country of a state of emergency and/or an appeal for international assistance. Only disasters designated as "storms" and "floods" are considered here, from which we obtain a monthly indicator variable per region if there was at least one natural disaster reported during a month.

[6] These types of events include tropical phenomena, storms, cyclones, damages due to waves or tidal waves, and floods. A natural disaster can combine several events of this type at the same time. The events we focus on notably excludes volcanic eruptions, damages due to lava, landslides, earthquakes, snow storms and avalanches, which are also reported in GASPAR.

Combining these two data sets, we have full information on natural disasters hitting one of the four regions as reported by administrative bodies. Table A.7 in the Appendix documents that most of the events in EM-DAT are also reported in GASPAR, but a smaller proportion of GASPAR events are reported in EM-DAT. This latter observation is due to the fact that GASPAR reports a significantly higher total number of events, which are as a result associated with lower intensity of economic losses.

Both data sources have well-documented reporting biases. A heterogeneous insurance pattern across French overseas territories likely leads to misreporting in the GASPAR database due to a charity hazard. Grislain-Letrémy (2018) shows that the probability that local authorities declare the state of emergency depends on the insurance coverage of households in their community. If this coverage is large, authorities have an incentive to declare an emergency, a pre-requisite in French law for insurance payouts. If the coverage is low, however, local communities might be better off calling for direct financial assistance from the French government. This imposes a misreporting bias into the GASPAR database. For EM-DAT, Felbermayr and Gröschl (2014) find a different bias. They conclude that news-driven and insurance-based data sets generally pose the problem of selection bias and a correlation of intensity measures with error terms in growth regressions. Such a selection bias would also most likely affect our results on inflation responses.

To overcome these potential biases, we complement our natural disaster data sets with information from meteorological records. This allows us to use an IV approach where reporting-based natural disaster events are instrumented by meteorological records (see the empirical specification below).

2.2.2 Meteorological records

We use three types of meteorological information as possible instruments: meteorological records (i) as reported by weather stations; or (ii) as collected by remote sensing systems based on satellites; and (iii) extreme weather events as reported by the French national weather service (Météo-France).

Meteorological records from weather stations are obtained from the Global Surface Summary of the Day (GSOD), a database derived from the Integrated Surface Hourly data set. This source provides data for over 9,000 stations around the world beginning in 1929, of which two to three match to each of the regions in our analysis (see Figure A.2 in the Appendix). Each weather station provides data on precipitation in 0.01 inches in cumulative terms per day and the maximum wind speed measured for one minute during the day in tenths of knots.

Figure 1. Data from remote sensing

a) Wind speed, Réunion

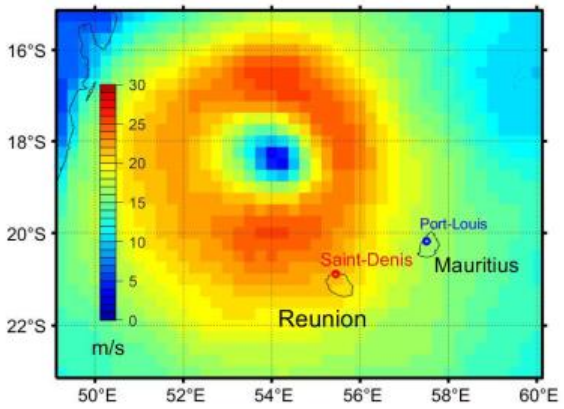

b) Precipitation, Guadeloupe

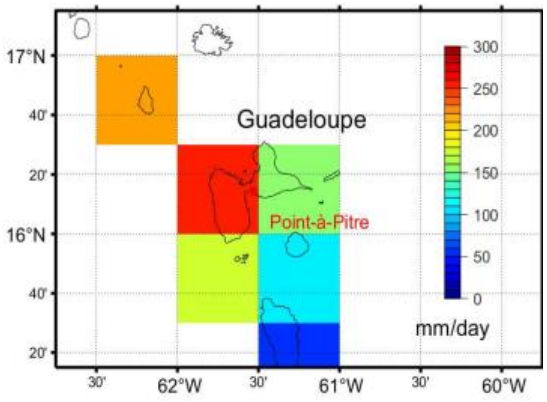

c) Wind speed, Réunion, Feb-2007

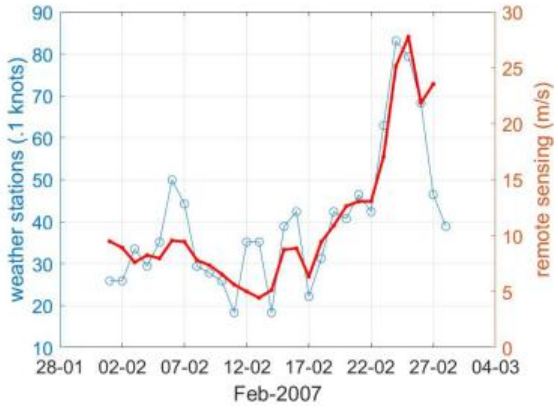

d) Precipitation, Guadeloupe, Nov-1999

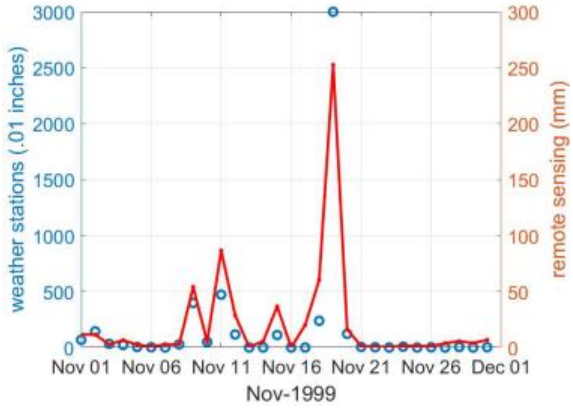

Note: Panel a: Wind speed via remote sensing from the NOAA Cross-Calibrated Multi-Platform (CCMP), measured on a 0.25-degree grid in meters per second on a range from 0 to 30. The panel shows the maximum average wind speed in a six hour interval in Réunion in the sample, which amounts to 27.76 m/s on 2007-Feb-25 (12AM) when cyclone Gamede passed the island. Panel b: Precipitation via remote sensing is taken from the NOAA Climate Prediction Center (CPC), measured on a 0.5-degree grid in millimeters per day. The panel shows the maximum daily precipitation in Guadeloupe in the sample, which amounts to 252.59 mm on 11.19.1999. Panel c: Wind speed records from remote sensing are plotted alongside the maximum for 1 minute sustained wind speed from weather stations as documented in the Global Surface Summary of the Day (GSOD) database in .1 knots. Panel d: Precipitation records from remote sensing are plotted alongside precipitation from weather stations as documented in GSOD in .01 inches.

We combine these data with meteorological records obtained via remote sensing. Wind speed is taken from the National Oceanic and Atmospheric Administration (NOAA) Cross-Calibrated Multi-Platform (CCMP) wind vector analysis that allows wind speed over the ocean surface to be computed in meters per second. Each vector summarizes the average wind speed in a cell of 0.25 degrees of latitude longitude coordinates within a six hour interval. Figure 1a provides an illustration of the data for the case of cyclone Gamede passing Réunion in February 2007. Precipitation data is taken from the NOAA's Climate Prediction Center (CPC) database, which provides daily cumulative precipitation in millimeters per square meter at a resolution of 0.5 degrees of latitude longitude coordinates. Figure 1b illustrates an episode of extreme precipitation in

Guadeloupe in November 1999 (see also Figures A.3 and A.4 in the Appendix). The data within each cell/day-observation or station/day-observation are aggregated to a region-month observation x_{it} using the maximum daily precipitation and wind speed observation, or $x_{it} = \max[x_{i1}, x_{i2}, \dots, x_{iN}]$, where N denotes the last day or the last six hour interval of month t in region i.

Compared with weather station data, remote sensing data has the advantage of providing an almost full coverage with relatively long historical data. However, the remote sensing data is also less reliable for extreme events, e.g. high wind speed (>15m/s). Table A.9 in the Appendix reports summary statistics calculated using the two different sources: overall, remote sensing data report lower precipitation levels than weather stations, and exhibit a lower variability. The opposite is true for wind speed data: remote sensing data reports higher wind speed and higher variability compared with weather stations. However, despite the different scales of remote sensing and weather station data, a direct comparison of records obtained through the wind speed event in Réunion in February 2007 (Figure 1c) and for rainfall in Guadeloupe during November 1999 (Figure 1d) shows that both measures detect the same day as an extreme event. Both types of records indicate that Réunion is the region with the highest average measure of wind speed, and that French Guiana is the region with the highest average measure of rainfall.

Lastly, we combine this continuous weather data with a dummy variable for all extreme weather events identified by the French national weather service (Météo-France), which lists 32 extreme meteorological events. 31% of events are located in Martinique, 25% in Guadeloupe, 25% in Réunion and 19% in French Guiana (see Table A.10 in the Appendix).

Figure 2 illustrates the correlation between administrative disaster data and the physical intensity of rainfall and wind. Specifically, it displays the occurrences of administrative events against the joint distribution of maximum monthly precipitation and wind speed, for data from remote sensing. Comparing discrete events with the physical intensity of wind and precipitation, it appears that a large number of events are located in the upper parts of the distribution. More specifically, EM-DAT and Météo-France events are almost systematically located above the median of either wind or precipitation records, and most of them are in the top quartile. Conversely, GASPAR events are mainly located in the center of the distribution. This reveals one of the main difficulties for empirical economic analysis of extreme weather events, which

is rooted in the imperfect correlation between the physical intensity of a meteorological event and economic damages. [7]

This suggests that events in the EM-DAT data set are related to natural disasters of significant physical intensity, while this is not necessarily the case for the majority of events from the GASPAR data set.

Figure 2. Administrative shocks and joint distribution of precipitation and wind speed

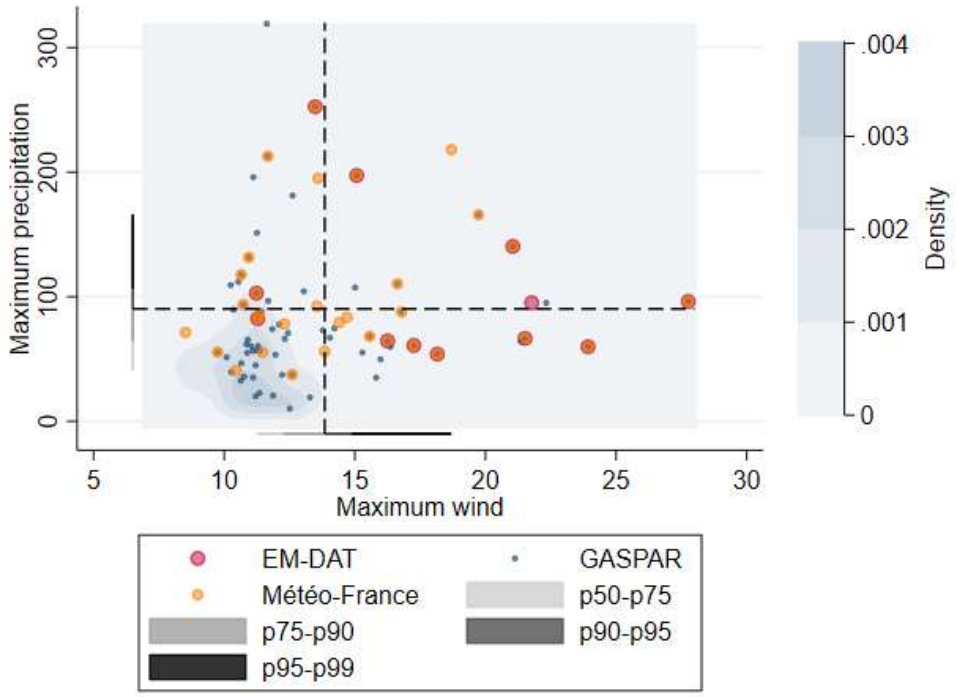

Note: Events from EM-DAT, GASPAR and Météo-France are illustrated as discrete events and plotted against the distributions of physical intensity of wind speed in meters/second from the CCMP (x-axis) and rainfall in cumulative millimeters per day from the CPC (y-axis). Dotted lines represent the median value of wind speed and precipitation across all four regions.

3. Empirical strategy

In this section, we describe our baseline empirical methodology to derive causal dynamic effects from extreme weather events that incur significant economic damages.

[7] This discussion also helps to distinguish between weather and climate. Following the literature, we would refer to climate as moments of the distribution underlying longer periods of realizations of weather data. Our focus is on extreme weather realizations in the tails of the distribution of precipitation and wind speed data recovered via remote sensing techniques, and not in effects of changes in the moment of this distribution (see e.g. Dell et al. (2012) for the latter).

3.1 Discussion on instrument validity

When we relate inflation directly to weather-related disasters as measured from administrative data sets, our estimates could eventually suffer from two types of bias. First, an attenuation bias can arise, e.g. if some natural disasters are reported while there is no substantial economic damage, or no underlying extreme meteorological event. Similarly, an omitted variable bias is also possible if reporting biases are systematic. Furthermore, the use of dummy variables alone does not allow a direct interpretation of the effects with respect to the intensity of the natural disasters. In our baseline empirical approach, we therefore instrument our weather-related disaster events using meteorological data. We propose using meteorological data as instruments for the intensity of economic damages incurred by weather-related disaster events. The success of the strategy depends on the validity for meteorological data to serve as an instrument, thus if our instrument is relevant and exogenous.

Instrument *relevance* is given under the implicit assumption that the intensity of rainfall or wind speed is correlated with the size of economic damages caused by meteorological events. Results from the first-stage regression in the next Section indicate a high relevance of meteorological data, in linear and non-linear specifications, with reported events that had significant economic cost. The computed F-statistics are generally close to or above 20, far above conventional rule of thumb levels for possibly weak instruments.

Instrument *exogeneity* is given if the weather-related disaster is unrelated to other shocks that effect the inflation rate in systematically the same way. In other words, weather-related extreme events should affect prices only through the economic damages they create. In this sense, we follow the literature and argue that natural disasters captured by meteorological data alone are plausibly exogenous to economic outcomes (Strobl, 2012, Felbermayr and Gröschl, 2014). However, we will argue below (Section 4.3) that due to a possible overlap of seasonality patterns in the outcome variable (inflation) and the instrument (meteorological records), it is important to include a rich set of regional seasonality dummies to insure instrument exogeneity conditional on inclusion of all control variables (Stock and Watson, 2018).

3.2 First-stage regression

In a first step, we regress our binary variable of administrative natural disasters $\omega_{i,t}$ on meteorological data $X_{i,t}$ for region *i* at date *t* (year-month) using the following specification:

$$\omega_{i,t} = \alpha + \beta X_{i,t} + \delta_t + \mu_m + \gamma_i + \mu_m \times \gamma_i + \varepsilon_{i,t}, \quad (1)$$

where γ_i is a region fixed effect, δ_t is a time (year-month) fixed effect, μ_m is a calendar month fixed effect. The motive for interacting regional fixed effects with a monthly dummy is that seasonality of weather shocks can differ across regions.

Table 1. First stage: Regressing administrative disasters on meteorological data

	Remote sensing data				Weather station data			
	(1)	(2)	(3)	(4)	(5)	(6)	(7)	(8)
Wind	**0.026*****	0.009	-0.047	-0.014	0.011	0.025	0.198	0.031
	(3.53)	(0.30)	(0.41)	(0.43)	(0.69)	(0.38)	(0.65)	(0.42)
Rain	**0.002*****	0.002*	0.002*	0.002**	0.001***	0.000	0.001	0.001**
	(4.28)	(1.90)	(1.74)	(2.28)	(4.32)	(1.06)	(1.30)	(2.07)
$Wind^2$		0.001	0.004	0.002*		-0.002	-0.062	0.000
		(0.51)	(0.57)	(1.66)		(0.21)	(0.61)	(0.04)
$Rain^2$		0.000	-0.000	0.000		0.000	-0.000	0.000
		(0.26)	(0.65)	(0.45)		(1.16)	(0.58)	(1.07)
$Wind^3$			-0.000				0.006	
			(0.49)				(0.61)	
$Rain^3$			0.000				0.000	
			(0.80)				(0.90)	
Météo-France event	**0.426*****	0.420***	0.425***		0.485***	0.485***	0.499***	
	(5.25)	(5.02)	(4.99)		(6.18)	(6.16)	(6.14)	
R^2	**0.35**	0.35	0.35	0.29	0.33	0.33	0.32	0.24
N	**928**	928	928	928	928	928	928	928
F-Stat	**39.68**	23.35	18.96	21.19	29.68	17.55	9.85	14.76

Note: Estimation results for first-stage model (2) with dependent variable all natural disasters reported in EM-DAT and GASPAR as binary variable. All wind speed variables are expressed in m/s and all precipitation variables are expressed in mm. *Wind* in columns 1-4 corresponds to the maximum wind speed from the CCMP database per region and month. *Rain* in columns 1-4 is the maximum daily precipitation in a region as reported by the Climate Prediction Center (CPC). *Wind* in columns 5-8 corresponds to the monthly maximum of sustained wind speed per region and month from GSOD. *Rain* in columns 5-8 is the maximum daily precipitation amount per month and region taken from GSOD. *MF* is a dummy variable for a noticeable event reported by the French national meteorological service Météo-France. T-stats are reported in parentheses. Significant at ***0.01, **0.05, *0.10.

Table 1 reports the results of first-stage regressions using meteorological data collected via remote sensing (columns 1 to 4) or data collected via weather stations (columns 5 to 8) as exogenous variables. In the different regressions, we consider linear (columns 1 and 5), square (columns 2 and 6) and cubic (columns 3 and 7) specifications of wind speed and precipitation. Non-linear terms for wind speed and precipitation are considered since there is evidence that economic damage from wind speed is best captured by a cubic relationship (Emanuel, 2011). Note that non-linearity is explicitly taken into account in all our specifications since we include Météo-France events as dummy variables in equation (1). In order to assess the impact of this

dummy on the coefficient of remote sensing and weather station data, we also present the square specification without including the Météo-France events (columns 4 and 8).

Some novel results emerge from this table. First, all specifications show a very strong first-stage relationship, with F-statistics typically above 20 for remote sensing data and above 10 for data from weather stations. This underlines the high relevance of meteorological data for particularly destructive disaster events in an IV setup. Second, overall, remote sensing data appear to have a higher predictive power (with F-statistics and R-squared systematically higher than for weather stations). This is a surprising result, as data from weather stations are known to be more precise for high wind speed and precipitation levels. However, the better coverage in terms of geography of remote sensing data and the uninterrupted availability at a daily frequency more than make up for this. When it comes to predicting an extreme weather event, the data quality is sufficient, as confirmed by Figure 1c and Figure 1d. Third, in all specifications, dummies for Météo-France events predict strongly and significantly the probability of an economically significant event. Removing dummies for Météo-France, as we do in columns (4) and (8), entails slightly more significant coefficients for non-linear terms (for instance, the square term of wind speed for remote sensing data becomes significant at the 10% level), but a lower adjusted R^2. Therefore, modeling the non-linearity between meteorological data and economically significant events through the inclusion of Météo-France dummies is favored over the inclusion of non-linear meteorological data.[8]

Based on these results, our preferred specification is that of column (1) from which we compute fitted values $\widehat{\omega}_{i,t}$. Since the dependent variable is an indicator variable associated with weather-related disaster events with large economic damages, we interpret $\widehat{\omega}_{i,t}$ as the predicted probability of an economically significant natural disaster as a function of meteorological data.[9] A one-standard deviation increase in wind speed (for an average standard deviation across regions of 1.7 meters per second) increases the probability of observing a natural disaster according to administrative data sets by 4.4 pp. Conversely, a one-standard deviation increase in precipitation level (for an average standard deviation across regions of 95.2 mm) increases the probability of observing a natural disaster according to administrative data sets by 19.0 pp. As a matter of comparison, the average predicted probability of a shock conditional on

[8] However, for applications in which the Météo-France data is unavailable, column (4) still highlights that the inclusion of non-linear terms is recommended.

[9] As we are in a linear setting, some predicted probabilities $\widehat{\omega}_{i,t,m}$ lie below zero and above 1, as illustrated by Figure B.1 in Appendix B.

observing no shock is 3%, while it is equal to 57% when conditional on observing a shock (the figures are the same if we condition only on GASPAR shocks, but they are respectively 6% and 86% if we condition on the occurrence of an EM-DAT shock).

Figure B.1 in Appendix B shows the distribution of predicted probability, and Figures B.2 to B.4 decompose the latter conditionally on actual administrative natural disasters, based on the specification of column (1). While the distribution of predictive probabilities is strongly skewed to the right, we observe that the distribution conditional on an observed administrative shock is shifted to the right compared with the distribution when there is no administrative shock.

In the rest of the paper, we present results based on the specification of column (1), and compare it with alternative specifications (notably using weather station data and different choices of time fixed effects).

3.3 Second-stage regression

Our estimation for the second stage relies on a local projection method (Jordà, 2005). We relate the log of the price index evolution between date *t-1* where *t* corresponds to the date (year-month), and date *t+h* where *h=0,...,6* months to the estimated probability of a natural disaster $\widehat{\omega}_{i,t}$ recovered from equation (1). The index i is for the different regions, $i = 1, \dots, 4$. Our baseline equation is the following:

$$\log\left(\frac{P_{i,t+h}}{P_{i,t-1}}\right) = \tau_h + \theta_h \widehat{\omega}_{i,t} + \gamma_{i,h} + \delta_{t,h} + \mu_{m,h} + \mu_{m,h} \times \gamma_{i,h} + \varepsilon_{i,t,h}, \qquad (2)$$

where $\widehat{\omega}_{i,t}$ is the predicted probability of a natural disaster at date *t* in region *i* according to administrative data sets. Time (year-month) fixed effects are denoted by $\delta_{t,h}$, while $\mu_{m,h}$ denotes calendar month fixed effects. Region fixed effects are denoted by $\gamma_{i,h}$, while $\varepsilon_{i,t,h}$ is an i.i.d residual. This equation is estimated separately for each horizon *h*, and the parameters of interest are θ_h, which capture the cumulative effect on prices of a natural disaster for each horizon h. $\mu_{m,h} \times \gamma_{i,h}$ is an interaction term to capture region-specific monthly seasonal variations.

In our main specification, we estimate equations (1) and (2) using a 2SLS estimator. We also compare the 2SLS estimates with OLS specifications in which we directly regress price variations on $\omega_{i,t}$, i.e. the dummy variable capturing the occurrence of an administrative shock. Given the descriptive statistics presented on natural disasters, we expect the estimated price

reactions to be stronger under the instrumental variable estimation than under the OLS estimation. The 2SLS estimate gives the variation of price reaction to the continuous linear predicted probability of an administrative shock that ranges from 0 to 1. Put differently, it gives estimates of prices reactions for administrative shocks that are triggered by extreme meteorological events, but not for those that are unrelated to the latter.

Our parameter of interest θ_h should be interpreted as the effect on inflation of an increase in the probability of observing the *average* discrete administrative shock triggered by an increase in an extreme meteorological event. However, since our approach relies on a continuous instrumental variable in the first stage, it also captures the intensive margin of a weather-related disaster. Even though the treatment is binary, the probability of observing the average treatment is increasing in the continuous meteorological records, and thus embeds some intensity effects (see also Section 5 for a more complete discussion).

Another important question related to this estimation strategy is how it compares with other methodologies used in the literature, and notably to the damage function approach. One potential concern about our IV approach is indeed that it might substitute biases of administrative data with measurement biases due to meteorological data. Besides, since their effects on economic activity are highly non-linear, the accuracy of the results depends on how well non-linearities are captured by our available measures of wind speed, rainfall and the extreme event dummy variable reported by Météo-France. In order to compare our IV approach with an alternative existing empirical strategy, we have also run an OLS regression where the exogenous variable is a standard damage function, as described in Heinen et al. (2018) (see section 4.2 for details).

4. Main results

In this section, we present the results of our baseline estimation strategy for both the OLS and IV approach, and compare them to alternative specifications.

4.1 Baseline specification

In Figure 3, we present the main results from our baseline estimations (OLS and IV settings) for headline CPI. Based on the IV estimation, our first main finding is that total CPI is on average affected by weather-related disasters. It first increases moderately and temporarily by about 0.5% after two months. The effect rapidly narrows down to zero. The OLS estimate

exhibits broadly the same pattern, but with much smaller coefficients (reaching a maximum of 0.06% after two months). These estimates for total CPI are in the range of those found in the existing literature. Heinen et al. (2018) find that an average hurricane or flood causes a temporary rise in CPI by about 0.1 pp. Parker (2018) finds that a natural disaster among the top quantile leads to an increase in total CPI of about 0.6 pp after a year, and 0.9 pp after two years.[10]

Figure 3. Main results – Headline CPI

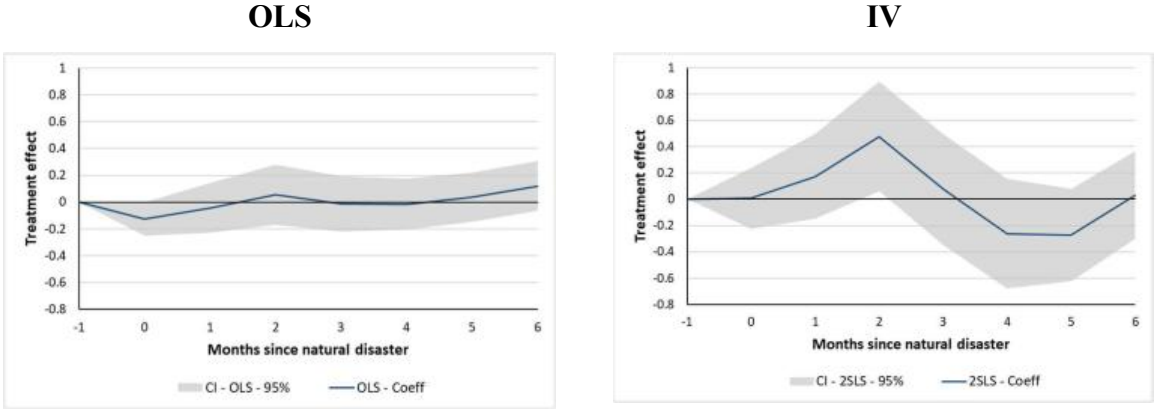

Note: The figures plot the cumulated impulse response function for headline CPI, in our baseline OLS and IV specifications. Treatment effects are expressed in percent. 95% confidence intervals with robust standard errors in the shaded areas.

Our second main result is that composition effects drive the impact on aggregate inflation, which vary over time. Figure 4 displays the estimated coefficients for the six main components of headline CPI, comparing our baseline 2SLS estimate with OLS estimates.[11] On the one hand, inflation of fresh products increases strongly and rapidly, up to 11% after two months. This effect is particularly strong, as it typically represents about 2.2 standard deviations of fresh food CPI on average across the four overseas territories. This positive effect then decays progressively, until reaching zero after six months. Weather-related disasters also have a positive effect on prices of other food items, but the magnitude of the effect is much smaller (+0.3%). On the other hand, prices of services and manufactured products decrease moderately by 0.2%. These effects are marginally significant (at the 10% level), slightly more persistent

[10] Both papers find that positive effects are stronger for food, and that the effects are generally negative for other components (such as housing). However, contrarily to our estimates, the effects cannot be decomposed as data on consumption weights are not available (Heinen et al., 2018) and data coverage is not homogenous across countries (Parker, 2018). Parker (2018) also finds that upward effects are more persistent for droughts and to a lesser extent for floods, but not for storms.

[11] The full set of estimated coefficients in the baseline 2SLS, both for headline CPI and its 12 subcomponents, is presented in Table B.1 in the Appendix. Figure B.5 and Table B.2 in the Appendix present the cumulated price response for OLS with confidence intervals. Finally, while we do not present results regarding pre-trends in our baseline results, we find them to be of small magnitude and largely insignificant (see Figure B.8 in the Appendix for the baseline results of fresh products with pre-trends up to 3 months).

than those observed for fresh food products, and broad-based across their subcomponents. Finally, prices of energy or tobacco do not react significantly to the natural disaster shocks, which is expected since they are strongly administered. In all specifications, 2SLS estimation yields higher estimates than the OLS estimation. In the case of fresh products, the maximum effects estimated in the OLS are positive and significant, but about 3.5 times smaller than those estimated in the 2SLS setting. This confirms that using only administrative shocks tends to underestimate the effects of disasters on inflation since many of these natural disasters (in particular as reported by the GASPAR data set) do not correspond to extreme meteorological events and are therefore likely to be related to lower real economic damages.

Figure 4. Main results – CPI components - IV

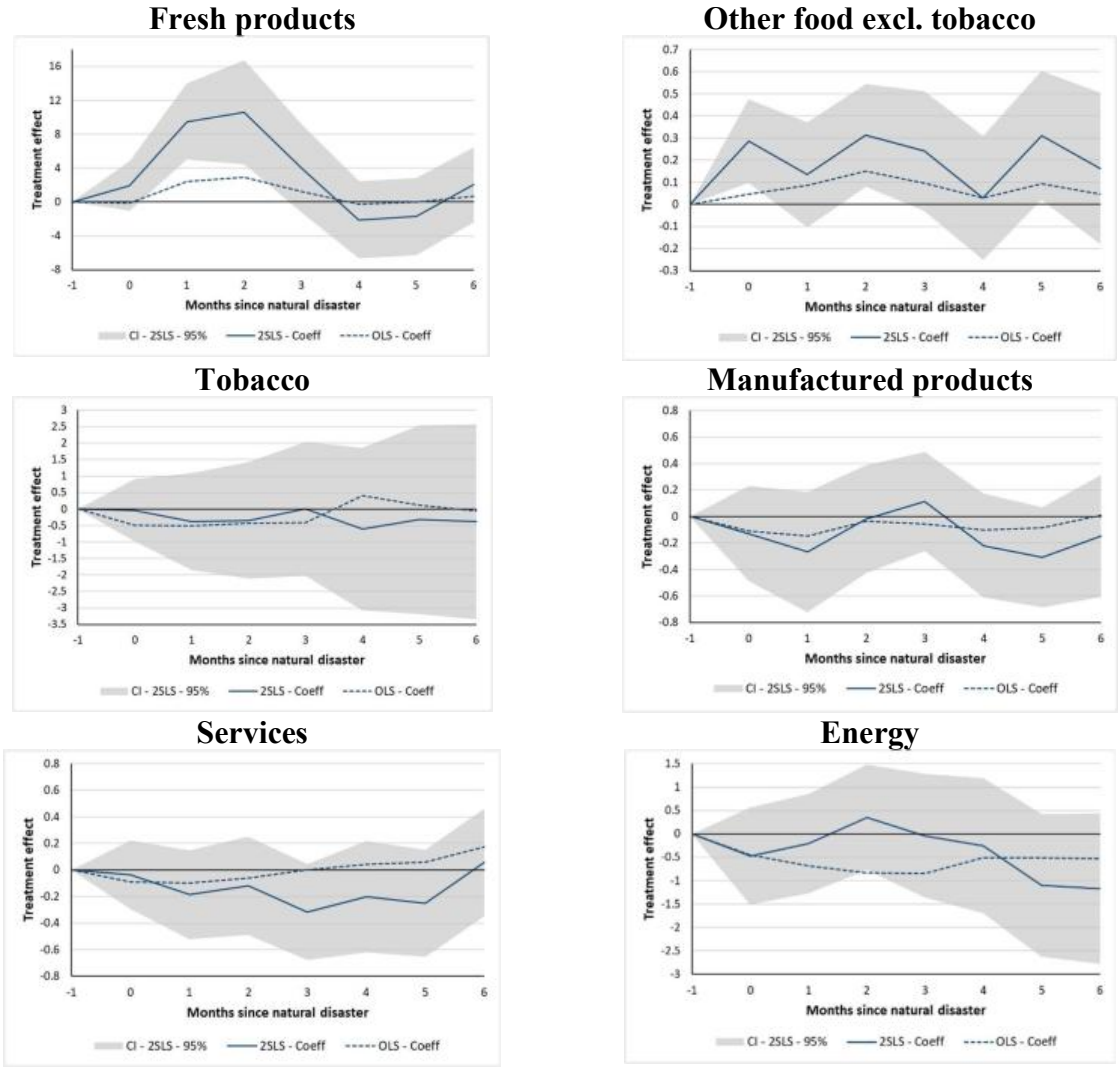

Note: The figures plot the cumulated impulse response function for headline CPI and its different subcomponents, in our baseline IV specification (solid blue) and for the OLS specification (dotted blue). 95% confidence intervals for the 2SLS specification with robust standard errors in the shaded areas. Treatment effects are expressed in percent.

Turning to the interpretation of these results, the positive effects on the prices of food are likely to be driven by supply-side factors, while the negative effects on other CPI items are likely to be driven by demand factors. To shed light on these mechanisms, we estimate reactions of sector-level employment in overseas territories to natural disasters. Results are reported in Table B.3 in the Appendix.[12] Our main finding is a sustained decrease in agricultural employment following a natural disaster (reaching a maximum effect of -3% after two months, but remaining around -1% to -2% after 6 months). This suggests that the price increase in food results from a negative supply shock related to the destruction of crops in fields. In parallel, we also observe an increase in the level of employment in other low-skilled jobs, such as in interim (reaching a maximum of 16% after 4 months, but remaining above 5% over the projection horizon), and in car repair (+1% after 5 to 6 months), suggesting some worker reallocation effects from agricultural sector to these sectors. This finding is in line with previous studies documenting a drop in agricultural labor supply after natural disasters (Kirchberger, 2017). This also suggests a stronger negative supply effect for fresh food products, which are more likely to be produced locally than for other food products, which are often imported. The supply of other items is likely to be less responsive to weather-related disasters, since these products are largely imported (manufactured products, tobacco and energy)[13] or produced through the public sector (services). Unsurprisingly, employment in these sectors does not react to natural disasters.[14] There is one exception, which is a significant drop in construction sector employment for three months, reaching up to -1.4 pp before fading out. However, it is difficult to map this sectoral drop in employment with inflation data by product type, as costs related to owner occupied housing are systematically excluded from HICP inflation in the euro area. Some home-related expenses fall under the two product categories "Other manufactured products" and "Other services" (Table A.4), both of which have falling inflation rates in response to weather-related disasters. This is consistent with potentially lower activity in the construction sector due to weather-related business interruptions. The combination of these factors with a downward price reaction points towards the predominance of negative demand effects.[15]

[12] We describe available measures of sectoral employment in overseas territories in the Appendix, Table B.3. These results should be considered as more exploratory than those on consumer prices, as they are based on quarterly data and are available for a shorter period of time.

[13] Regarding energy, the prediction is, however, that supply and demand effects are less relevant than for other components of the CPI. First, in France, oil prices quickly follow the international prices of crude oil (Gautier et al., 2023), making unlikely that local supply or demand effects affect the general price dynamics. On the other hand, in the specific case of DROMs, oil prices are set administratively, which might mute the effects of any existing supply or demand effect. The negative effect of natural disasters on energy prices is therefore hard to interpret.

[14] Relatedly, we did not find any effect of natural disasters on the value or volume of imported goods.

[15] In the case of services, comparing the variation of economic activity in the tourism sector with accommodation and restaurant prices would be particularly useful. However, while we observe employment and activity in the accommodations/restaurants sector, we do not observe the CPI of accommodations and restaurants (which is part of the "other services" aggregate). Interestingly, we observe no employment variation in the tourism sector, but find an immediate increase of about 10 % in the

This result is in line with recent contributions showing that natural disasters decrease demand, notably through higher risk aversion (Cantelmo et al., 2023 and Cassar et al., 2017).

Figure 5 decomposes the effect on total inflation based on the observed effect for the five main components (namely fresh food, other food including tobacco, services, manufactured products and energy) using the results of the IV estimation. Each contribution is computed as the observed pass-through multiplied by the average weight of the component over 1999-2018. The "residual" contribution corresponds to the difference between the estimated reaction of headline inflation and the sum of estimated contributions of the five components. The response of inflation to weather-related disasters is heterogeneous across CPI components both in terms of timing and amplitude, with a quick and positive response from food inflation (especially fresh food), and a negative contribution of inflation in services and manufactured products.

Figure 5. Decomposition of the reaction of total inflation in the baseline specification

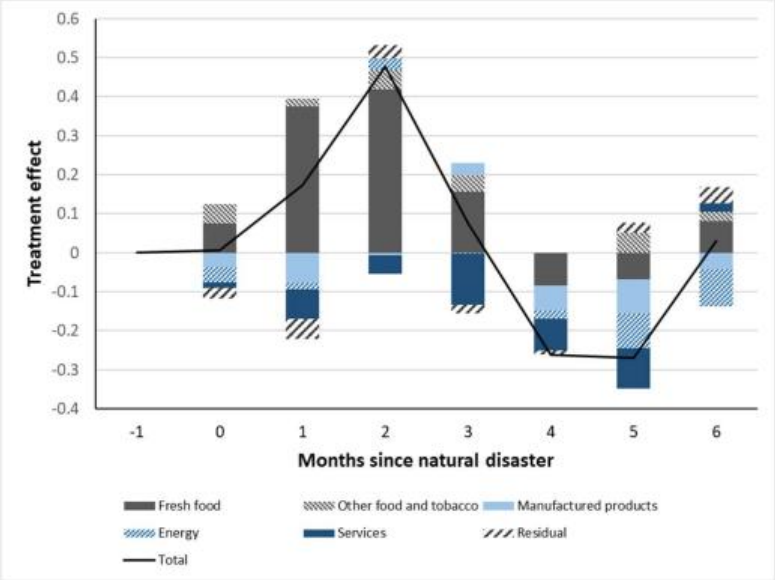

Note: Decomposition of the cumulative impulse response of headline CPI to a natural disaster in the baseline IV local projection. The contribution of each component is computed as the cumulative response of the CPI of this component times its average weight in the consumer baskets of the four overseas regions between 1999 and 2018. Treatment effects are expressed in percent.

number of overnight hotel stays, which progressively vanishes. This points to a positive demand shock, which could be driven by relatives coming to help their family in the aftermath of the disaster (in a context where the majority of tourism flows in overseas regions are due to affinity motives). Another explanation could be that hotels were used as temporary accommodation for households who lost their homes.

4.2 Comparison with results from damage functions

In this section, we compare our baseline results to two different sets of estimates obtained with damage functions. In a first step, we construct damage functions from remote sensing data in close analogy to Heinen et al. (2018). Damage functions represent a mapping from weather or climate into economic outcomes in the sense of a "dose response function" (Auffhammer 2018).

For the wind destruction index, we follow Strobl (2012), who builds a hurricane destruction index. We adjust his approach for the use of remote sensing data of wind in order to obtain a time-series of wind damage for each region. Specifically, for gridded cell *j* of weather data in one of our four regions *i* and within a day *d*, we compute the monthly wind-destruction as

$$H_{it} = \max\left[\sum_{j=1}^{J} \xi_{ij} \sum_{d=1}^{D} \left(W_{ijd}^{max}\right)^3 \times \mathbb{1}_{\{W_{ijd}^{max} > W_i^*\}}\right]_{d \in t}, \quad (2)$$

where ξ_{ij} are exposure weights for grid cell *j* in region *i*, which aggregate to one at the regional level, W_{ijd}^{max} is the maximum sustained wind speed for one minute in an intraday window *d* of six hours from the CCMP, and $\mathbb{1}_{\{W > W_i^*\}}$ is an indicator variable that takes the value of one if the recorded wind speed exceeds a threshold value W_i^*. Maximum sustained wind speed enters the damage function in cubic form, as it has been found that the local destructive power of wind is roughly in cubic form related to wind speed (Emanuel 2011).

Exposure weights ξ_{ij} are constructed from satellite nighttime light data. Nighttime light has a high predictive power for economic activity and can usefully complement official statistical data (Henderson et al., 2012). Pérez-Sindín et al. (2021) show that nighttime light is a good proxy for regional GDP patterns in Colombia independent of the level of urbanization, which ranges in their study from rural areas with less than 5,000 inhabitants to cities of more than 500,000 inhabitants. Chen and Nordhaus (2019) show that satellite nighttime light data is better at predicting cross-sectional GDP than time-series evolutions of GDP, which makes it particularly suited for the construction of weights in our application, as we are only interested in detecting areas of relatively higher economic activity.

Regarding possible economic destruction due to excessive rainfall, we also follow Heinen et al. (2018) and define region-specific flood destruction as

$$F_{it} = \max\left[\sum_{j=1}^{J} \xi_{ij} \times r_{ijdt} \times \mathbb{1}_{\{r_{ijdt} > r_i^*\}}\right]_{d \in t}, \quad (3)$$

where r_{ijdt} is the cumulative sum of rainfall in millimeters over a three-day window in region *i*, weather cell *j*, on day *d,* in month *t*. The exposure weights ξ_{ij} follow the same logic as above and are also constructed from satellite nighttime light data (see Appendix C for details on the calibration of region-specific threshold values r_i^*).

In Figure 6, we compare our baseline estimates for total CPI and fresh products CPI to estimates using damage functions. Since the units of the damage function are not directly comparable to those of the explanatory variable in the second stage of our baseline 2SLS (which is a predicted probability), we present predicted price responses for two distinct variations of damage functions. The first one corresponds to the slope of the regression of the predicted probability on the damage functions, i.e. the variation of damage functions associated to a predicted probability going from 0 to 1. In that case, the inflation response is directly comparable to our baseline 2SLS. The second case does not use the predicted probability, and corresponds simply to the difference between the top percentile of damage function and the first percentile, i.e. the price response when damage functions shift from their 1% lowest value to their 1% top value. In both cases, the plotted predicted price response is the cumulative predicted price response for each damage function.

Figure 6. Damage functions for total CPI and for fresh products CPI

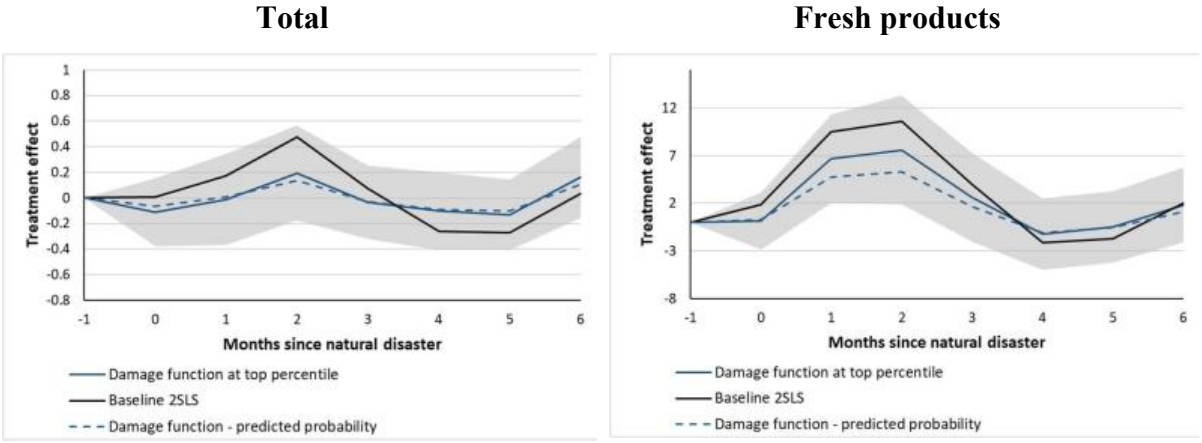

Note: The figures plot the cumulated impulse response function for damage functions evaluated using the predicted probability of shock (dotted blue) or at the top percentile of damage function (sold blue), compared to our baseline 2SLS (black line). Shaded areas represent 95% confidence intervals with robust standard errors for damage functions evaluated at the top percentile of shocks. Treatment effects are expressed in percent.

The results using this specification are very coherent with those of our baseline 2SLS methodology. Both estimated reactions appear to be close, and the price reaction using the damage function appears slightly smaller than that obtained in our baseline specification. In particular, the price reaction in our baseline 2SLS is higher than the price reaction of damage functions estimated at its top percentile: this suggests that our estimation is unlikely to underestimate price reactions compared with damage functions. In Figures B.6 and B.7 in the Appendix, we report results of separated regressions for the wind damage function and rain damage function, both evaluated at the top percentile. Results appear to be mainly driven by the wind damage function, with only limited effects from the rain damage function, a result that is similar to those obtained by Heinen et al. (2018).

Table 2 – Alternative specifications for the 2SLS strategy

	T=0	T=1	T=2	T=3	T=4	T=5	T=6
(A) Baseline							
Headline	0.01	0.17	0.48**	0.08	-0.26	-0.27	0.03
Fresh products	1.89	9.48***	10.60***	3.96	-2.11	-1.72	2.03
Other food excl. tobacco	0.29***	0.13	0.31***	0.24*	0.03	0.31**	0.16
Manufactured products	-0.13	-0.27	-0.02	0.11	-0.22	-0.31	-0.15
Services	-0.03	-0.19	-0.12	-0.32*	-0.20	-0.25	0.06
Energy	-0.48	-0.20	0.35	-0.04	-0.25	-1.10	-1.17
Tobacco	-0.04	-0.38	-0.35	0.00	-0.60	-0.32	-0.38
(B) No seasonal effect							
Headline	0.00	0.19	0.48**	0.26	0.17	0.16	0.22
Fresh products	7.66***	18.34***	20.86***	13.32***	3.56	-1.51	-2.46
Other food excl. tobacco	0.17**	0.07	0.19*	0.13	0.04	0.32**	0.25
Manufactured products	-0.59***	-1.11***	-1.26***	-1.13***	-1.00***	-0.72***	-0.69**
Services	-0.21	-0.24	0.13	0.51**	1.21***	1.36***	1.53***
Energy	-0.69	-0.99**	-1.00*	-1.65***	-1.84***	-2.15***	-1.98***
Tobacco	-0.10	-0.45	-0.72	-0.65	-1.01	-0.13	0.44
(C) No month-year FE							
Headline	-0.01	0.18	0.52**	0.25	-0.04	0.01	0.22
Fresh products	1.37	8.99***	11.40***	4.60	-0.23	0.18	2.62
Other food excl. tobacco	0.07	0.06	0.18	0.07	-0.16	0.22	0.07
Manufactured products	-0.04	-0.26	-0.06	0.17	-0.14	-0.23	-0.04
Services	-0.16	-0.37**	-0.20	-0.27	-0.26	-0.31	-0.10
Energy	0.04	0.82	1.50	1.54	2.18*	2.17	2.07*
Tobacco	0.41	-0.19	0.03	0.38	-0.31	-0.54	-0.93

***Note*:** The table shows alternative specifications of local projections of consumer prices in a 2SLS setting. Panel (A) shows results for our baseline specification, panel (B) shows results for a 2SLS specification controlling for year-month fixed effects, but not for region-specific month fixed effects and panel (C) shows results for a 2SLS specification controlling for region-specific month fixed effects, but not for year-month fixed effects.
*p < 0.10; **p < 0.05; *** p < 0.01.

4.3 Controlling for regional seasonality

Weather-related extreme events in overseas territories are often related to hurricanes and cyclones. The occurrence of storms is favored during periods when the difference between air

temperature and sea surface temperature is at its peak, resulting in seasonality. This matters for two reasons. First, it highlights the need to model regional seasonality in the empirical framework in order to prevent possible omitted variable bias. Second, instrument exogeneity requires that instruments and outcome variables are uncorrelated conditional on all control variables. Possibly overlapping seasonality between inflation and wind speed can be controlled for with regional month dummies. Next, we discuss sources and patterns of seasonality in the data and show how the treatment of this seasonality affects quantitatively our results.
Seasonality in extreme weather events differs across the territories.

Réunion is located in the South-West Indian Ocean, where the cyclone season is from December to April. Table A.8 in the Appendix shows that weather-related disasters in Réunion are indeed concentrated during the first half of the year. In contrast, Guadeloupe, Martinique and French Guiana are located in the northern hemisphere, while only Guadeloupe and Martinique are affected by the North Atlantic hurricane season, which is from June to November. Consistently, extreme weather events in these three regions are concentrated in the second half of the year. While Guadeloupe, Réunion and Martinique have a comparable number of administrative shocks (both in GASPAR and in EM-DAT), French Guiana has a much smaller number of shocks (all based on GASPAR data), which are mainly concentrated in the month of May (Tables A.7 and A.8).

Similarly, seasonal patterns in inflation differ across overseas territories. Figure A.1 in the Appendix plots the average monthly variations for the main components of CPI across regions. Seasonal variations in Réunion appear to be distinct from those of other overseas regions, both in terms of timing and in terms of magnitude. The difference of timing can largely be explained by the fact that Réunion is the only region in our sample located in the southern hemisphere, which affects the calendar regarding harvesting of local crops and tourism. The differences in the magnitude of seasonal variations between Réunion and other regions are particularly salient for fresh food and services, the latter likely driven by seasonality in the tourism sector.

In our baseline regression, we have included month fixed effects interacted with regional fixed effects to capture the seasonal effects specific to each region. In this section, we compare our baseline 2SLS specification with alternative 2SLS specifications controlling differently for seasonal patterns. Table 2 reports the results. Panel (A) reports our baseline estimates. Panel (B) reports results from a specification excluding monthly region-specific fixed effects (but including month-year fixed effects common to all regions). Panel (C) reports results from a

specification excluding month-year fixed effects (but including monthly region-specific fixed effects and year fixed effects common to all regions). While the effects for headline CPI remain very comparable across specifications (with a maximum estimated effect of 0.5% after two months), the product-level price reactions differ substantially. In particular, not controlling for region-specific monthly seasonality yields much stronger effects for fresh food products (which go up to 21% after two months). This is driven by the distinct seasonality of Réunion, which is the only overseas region located in the southern hemisphere, and for which the magnitude of seasonal variations of fresh food prices is higher than in other areas. These stronger effects for fresh food products are offset by stronger negative effects for manufactured products (down to a minimum of -1.3% after two months), and on energy (down to -2.1% after 5 months). Additionally, the prices of services increase more substantially at the end of the horizon (up to 1.5% after 6 months).[16] Controlling for seasonal effects (but not for time fixed effects), yields results closer to our baseline specification (with a maximum reaction of fresh food products of 11%, and a more significantly negative reaction of services prices after two months). However, it implies a positive reaction from energy prices, which is hard to reconcile with the fact that energy products are imported.

Overall, these results imply that controlling for region-specific seasonal patterns is quite important for the precise and unbiased estimation of dynamic causal effects of weather-related extreme events on prices.

5. Distributional effects of natural disasters

5.1 Which households are worst affected by natural disasters?

In this section, we investigate whether the effects of natural disasters on consumer prices vary across different types of households. Indeed, given that the main positive effects on inflation are channeled through fresh food products, and to the extent that the weight of food is generally higher for households with a lower income, we expect that the effect on total inflation is higher for the latter. To test this hypothesis, we use data from a survey produced by INSEE for 2017 (*Budget des familles*). This survey gives a decomposition of the consumption basket of households, both across overseas territories and across quintiles of household.[17] We combine

[16] This specific effect appears to be entirely driven by the disasters and price seasonality of French Guiana, in which 60 % of shocks occur in the month of May.

[17] Table D.1 in the Appendix reports the share of food in the consumption basket for each of the four regions we focus on, and confirms that the share of food decreases strongly when income rises.

these data with our estimated impulse-response functions, in order to derive an estimated impulse-response function of total CPI for each quintile (see Appendix D for the detailed methodology).

In Figure 7, we plot our estimated impulse response function of total CPI for each quintile, compared to the reconstitution of the impulse response function under average weights of fresh products between 1999 and 2018. Our results suggest that the maximum reaction of CPI in the first two quintiles is higher than the maximum reaction of CPI by about 0.1% for households, reaching about 0.6% after two months, against 0.5% in the effect estimated based on average weights. On the contrary, the reaction is more muted for households in the top of income distribution, notably those in the last quintile (maximum of 0.4 %).

Figure 7. Baseline and alternative effects on CPI inflation by income quintile

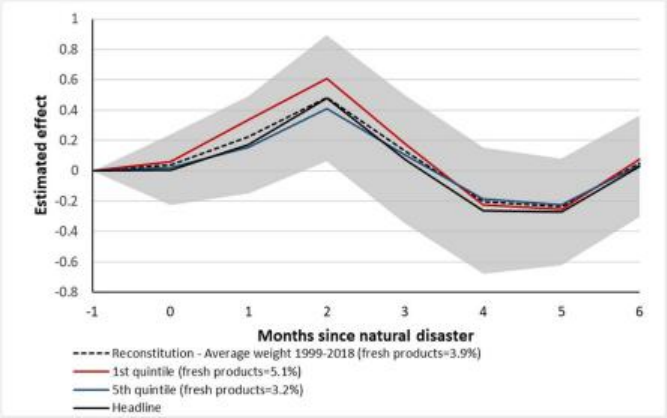

Note: Baseline 2SLS estimate for headline CPI in solid black, with its 95% confidence interval in the shaded area. The black dotted line is the reconstitution of the effect on headline CPI of using a linear combination of estimated effects on fresh products and total excluding fresh products using average weights between 1999 and 2018. The blue and red lines are the reconstitutions using estimated weights of fresh products for the top and bottom quintiles of income. Treatment effects are expressed in percent.

5.2 Do price caps help?

The extent of administered prices and local price control policies can affect the impact of natural disasters on prices. As argued above, one of the potential reasons behind the insignificant reaction from energy prices, beyond the fact that they are largely driven by international prices of crude oil, is that they are partly controlled by local authorities. However, more interestingly in our context, the extent of price regulation regarding food prices has also evolved over time. In November 2012, following protests against the cost of living in several overseas regions, a price cap (BQP – the *Bouclier Qualité Prix*) was implemented for a selected basket of elementary consumer products. The BQP, which was eventually implemented in March 2013, dictates that the total price for this basket of selected products cannot exceed a fixed ceiling.

The selection of products and the overall price cap are renegotiated annually, and can differ across regions. For example, in 2018, the BQP in Réunion contained 109 products for an overall price cap of 288 euros. 78 of these 109 products were food products, and among them, 48 were locally produced. The BQP can therefore be interpreted as a form of regulation to prevent price gouging.

Figure 8. Reaction of the fresh products CPI before and after the implementation of the BQP

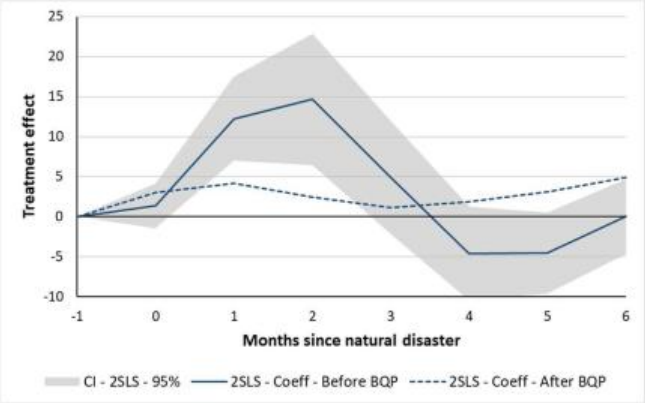

***Note**:* Impulse response functions of fresh food products for shocks occurring before the implementation of the BQP (until December 2012) and after the implementation of the BQP (from January 2013 onwards). 95% confidence intervals with robust standard errors in the shaded areas. Treatment effects are expressed in percent.

In Figure 8, we document cumulative impulse response functions for the prices of fresh products before and after the implementation of the BQP. In this case, we consider that the pre-BQP period is until December 2012, and that post-BQP period starts in January 2013.[18] Before the implementation of the BQP, the price reaction of food products was immediate and strong, reaching 12% after 2 months, and then decreasing to zero after four months. After the implementation of the BQP, the price reaction of fresh food products was much more sluggish, reaching 4% after one month and remaining between 0% and 5% over the whole projection horizon. As a result, the price reaction after the implementation of the BQP is significantly lower in the first few months, but significantly higher in the following months. Eventually, after six months, the cumulative price responses before and after the BQP are close (24% in the former case, and 20% in the latter), suggesting that the overall effect is similar in the long run, but the adjustment is smoother and more persistent with BQP than without. Overall, these effects therefore suggest that some amount of price gouging is likely to drive the price reaction in our baseline specification (as the maximum price variation is higher without regulation), but

[18] This evaluation is imperfect since it only compares two periods, during which several confounding factors could occur. However, the predictive power of the first stage is strong in both cases (F-statistic of 32.8 before the BQP and 13.0 after the BQP), and the number of shocks occurring annually in the regions during the two periods is very close (about 0.9 on average every year).

that it is unlikely to drive all of the price reaction. In the longer run, the cumulative price variations are identical with or without regulation, suggesting that retailers are constrained to increase their prices.

6. Robustness analysis

6.1 Quantifying the intensive margin in an IV setup

In this section, we present an approach to capture intensity effects in an IV setup. To do so, we implement the following strategy: we estimate the price response to a set of discrete shocks, where the shock is equal to one if the estimated probability based on equation (1) is above a certain threshold, and zero otherwise. We estimate these equations for a set of 928 evenly-spaced thresholds going from the minimum to the maximum values of estimated probabilities, and plot the estimated coefficient at horizon $h=2$ for each regression against the threshold probabilities. We compare these results with the one obtained in our baseline specification, and highlight the result based on an optimal discrete threshold according to a ROC criterion (i.e. a discrete shock based on a threshold probability that maximizes the share of true positives and minimizes the share of false positives).[19] Figure 9 plots the results for fresh food products.

Several conclusions can be derived from this figure. First, the maximum estimated effect based on discrete shocks derived from estimated shock probabilities increase in the threshold. The effect goes from about 0 when the threshold is equal to 0 (meaning that virtually all observations are defined as a "shock") to about 35% when the threshold is equal to 1 (meaning that only observations with the highest shock probability are treated as shock). Second, the estimated effect based on an optimal threshold derived from a ROC curve is only 4%. This comes from the fact that, while the predicted shock correctly identifies the majority of actually observed administrative shocks, a majority of predicted shocks actually do not correspond to an extreme weather event. Third, our baseline estimate is about 2.5 times the value of the estimate under the optimal threshold, and it is located in the upper part of the distribution (Figure E.2, Appendix). Indeed, even though it is largely below the maximum estimated value (35%), the number of estimations for which we observe an effect higher than our baseline is actually small (5.6%). Finally, we find that when the threshold of the predicted probability is set a little above

[19] See Appendix E for a description of how we derive this optimal discrete shock and its properties.

50%, the impact of natural disasters on prices of fresh food products varies around the value estimated in our baseline regression (about 10%).

Figure 9. Price reactions of fresh products for a set of discrete shocks based on varying thresholds of estimated probabilities

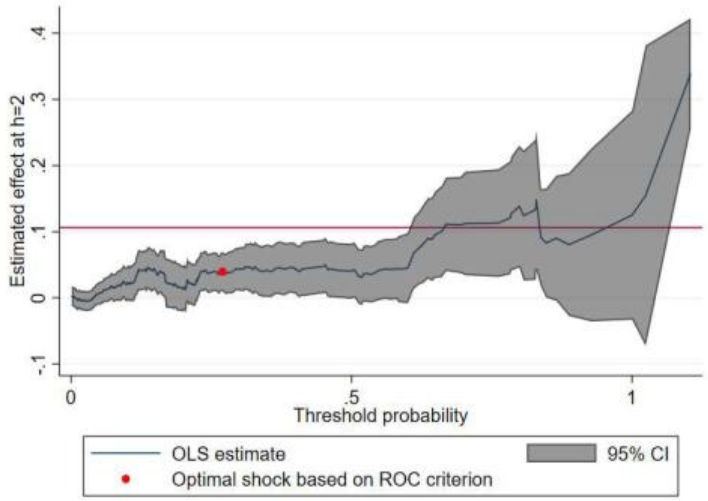

***Note**:* Maximum estimated effect of OLS regressions for fresh product prices with shocks based on discretized probabilities estimated from first-stage regression (1), with threshold varying from 0 to 1. Confidence intervals at the 95% level in grey. The red dot represents the estimate based on a threshold derived from a ROC curve. The red line corresponds to our baseline estimated effect.

6.2 Placebo regressions

In this section, we present results of different placebo regressions where we have randomized weather-related disaster shocks in both equations of our two-step model. We have run three distinct exercises.

In a first exercise, we randomize the instrumental variables. Namely, we simulate rainfall and wind data from Gumbel laws of distribution (whose parameters are derived from the empirical distribution of rainfall and wind records across regions) since the Gumbel law is well suited to replicate the distributions of extreme events. We also simulate Météo-France shocks from a uniform distribution, drawing as many shocks as the actual number of observed Météo-France shocks in our data, but without allocating them to regions in proportion to their observed frequency of shocks. We run 100 2SLS estimations, each based on a distinct set of simulated data for instruments and using the actual observations for the treatment variable.

In a second exercise, we keep the actual values of the instrumental variables, but we randomize the treatment, drawing randomly 69 shocks from a uniform distribution. As in the previous exercise, we do not allocate them to regions in proportion to their observed frequency of shocks.

We run 100 2SLS estimations, each based on a distinct set of simulated data for the treatment, but keeping the actual observations of the instrumental variables (see Appendix F for further methodological details).

In a third exercise, we keep the actual values of the instrumental and treatment variables, and we compute the correct predicted probability of treatment in the first stage, but we randomly allocate this predicted probability across regions and over time between the first and second stage. We run 100 OLS estimations of the second stage, each based on a distinct set of randomization of the predicted probability.

Figure 10. Distribution of T-stats of placebo regressions

a) Randomization of instrumental variables | **b) Randomization of treatment variable** | **c) Randomization of predicted probabilities**

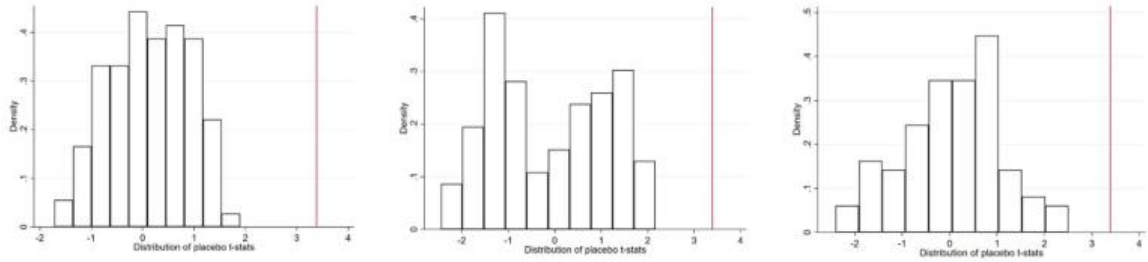

***Note*:** The figures plot the distributions of T-stats of placebo tests. In Figure 10a, the randomized variables are the instrumental variables. In Figure 10b, the randomized variable is the treatment variable. In Figure 10c, the predicted probability is randomly allocated across regions between the first and the second stage. The red vertical lines correspond to the t-stat of the baseline estimation.

Figure 10 plots the distributions of T-statistics for local projections of fresh food prices at horizon $h=2$, as well as the T-statistics from our baseline estimate (red vertical line). While the T-stat of the baseline estimate is equal to 3.4, 95% of those in the placebo estimates with randomization of instrumental variables are below 1.3 (Panel a), 95% of those in the placebo estimates with randomization of the treatment variable are below 1.7 (Panel b), and 95% of those in the placebo estimates with randomization of predicted probabilities are below 1.8 (Panel c).

6.3 Robustness to alternative specifications

In this section, we present several robustness exercises for headline CPI and the CPI of fresh products. Our robustness tests show that our main results hold and are robust to the chosen specification or to the definition of the shock, even if the exact magnitude of the effect can vary. The results are summarized in Table 3. Table B.4 in the Appendix presents results for the other components.

First, Réunion might play a specific role because the volatility of fresh food inflation is much higher there than in the other overseas regions, and also because extreme weather events are also more frequent in Réunion. When we estimate our baseline 2SLS without Réunion ("2SLS – Baseline – no Réunion"), the effect on headline CPI is still positive but insignificant, with a maximum of 0.2% after two months. The effect on prices of fresh products is much smaller than in the baseline (2.9%), but significant at the 5% level. Importantly, the identification power in the 2SLS setting is comparable to the baseline (the F-statistic of the first stage is of 21.6), which suggests that the lower estimated effect is not due to a lower quality of the model. This exercise suggests that most of the inflation effect of weather-related disasters comes from Réunion where extreme weather events are more frequent than in other regions.

Table 3 – Robustness analysis

	T=0	T=1	T=2	T=3	T=4	T=5	T=6
(A) Total							
2SLS - Baseline	0.01	0.17	0.48**	0.08	-0.26	-0.27	0.03
2SLS – Baseline – no Réunion	0.10	0.18	0.13	-0.09	-0.21	-0.29	-0.17
2SLS – Baseline, 3 lags shock	0.00	0.21	0.52**	0.15	-0.11	-0.12	0.18
2SLS – 3 lags CPI	-0.02	0.09	0.35*	-0.06	-0.41**	-0.39**	-0.10
2SLS – Baseline excl. shock < 6months	0.02	0.24	0.63**	0.10	-0.34	-0.35	0.04
2SLS – 6 lags forward	-0.07	0.13	0.42*	0.04	-0.34	-0.34*	-0.09
2SLS – Baseline, weather station data	-0.10	0.02	0.30	-0.01	-0.26	-0.33*	0.00
(B) Fresh products							
2SLS - Baseline	1.89	9.48***	10.60***	3.96	-2.11	-1.72	2.03
2SLS – Baseline – no Réunion	0.74	2.85**	2.53	0.38	-1.55	-1.08	0.35
2SLS – Baseline, 3 lags shock	2.16	8.93***	9.90***	3.39	-1.95	-1.17	2.60
2SLS – 3 lags CPI	2.37	9.78***	10.14***	2.82	-3.12	-2.70	1.14
2SLS – Baseline excl. shock < 6months	2.57	12.48***	13.91***	5.20	-2.70	-2.18	2.78
2SLS – 6 lags forward	2.17	9.87***	11.31***	4.08	-2.86	-2.13	2.02
2SLS – Baseline, weather station data	0.66	7.13***	9.19***	4.11	-0.77	-1.13	2.23

***Note*:** The table shows alternative specifications of local projections of consumer prices. Panel (A) shows results for total CPI, panel (B) shows results for the CPI of fresh products. "2SLS baseline" is our baseline 2SLS specification. "2SLS – Baseline – no Réunion" is the baseline specification excluding Réunion. "2SLS – Baseline, 3 lags shock" controls for up to 3 lags of the shock (instrumented by relevant lags of the instrumental variables). "2SLS – 6 lags forward" controls for up to 6 forward lags of the shock. "2SLS – 3 lags CPI" controls for 3 lags of monthly variations of CPI. "Baseline excl. shock < 6 months" is the baseline specification, excluding shocks that occur less than 6 months after a previous shock. "2SLS – Baseline, weather station data" is the baseline specification, but with instruments taken from weather station data rather than remote sensing data.
*p < 0.10; **p < 0.05; *** p < 0.01.

Second, we present alternative specifications in which we control differently for lags of the shocks and of the dependent variable. In a first specification, we control for up to three lags of the shock ("2SLS – Baseline, 3 lags shock"), instrumenting them with their respective lags of meteorological data. The estimated effect for fresh products is very close to our baseline specification, with a maximum effect of 10% after 2 months. In another exercise ("2SLS – 3 lags CPI"), we implement a lag-augmented local projection, as advised by Montiel-Olea and

Plagborg-Møller (2021), by controlling for up to three lags of CPI. Here again, the results remain very close to our baseline estimate.

Third, we run specifications taking into account the fact that shocks might occur at close intervals. In such a setting, our specification (which entails two-way fixed effects and prolonged treatment effects) might wrongly identify heterogeneous effects over time (as documented by De Chaisemartin and d'Haultfoeuille, 2020). In a robustness exercise, we first run a specification in which we do not define as a shock any event that occurs less than six months after a preceding shock ("2SLS – Baseline excl. shock < 6months"). Doing so, we find effects for fresh products that are of similar magnitude to those in the baseline specification, but slightly higher (12.5% after two months). Alternatively, in order to further rule out the risk that our results are potentially driven by compound effects, we control for up to six forwards of the shock. Here again, the results are robust, and if anything slightly stronger than in the baseline specification (effect of 11% after two months).

In a final exercise ("2SLS – Baseline, weather station data"), we present results using meteorological observations from weather stations in the first step. The maximum estimated effect on fresh products (7%) is very close to the baseline effect, yet slightly smaller, which confirms the lower identification power of data coming from weather stations.

6.4 Varying the share of fresh food

The overall positive effect of natural disasters on inflation is mainly driven by the large effect on prices of fresh food products, which represent a small fraction of the CPI basket of goods (4% on average between 1999 and 2018). The share of fresh food products has continuously decreased over our sample period from 5.9% in 1999 to 1.6% in 2018 (Table A.5 in the Appendix). In this robustness exercise, we estimate the overall effect on inflation of natural disasters when we vary the share of fresh products.

In Figure 11, we show counterfactual effects on headline inflation, assuming different weights for fresh products. The dark solid line represents the effect estimated in the baseline specification for total CPI, as estimated in Figure 3. The dark dotted line represents a reconstitution of the effect on total CPI, computed as a linear combination of effects estimated on fresh products and total excluding fresh products, using their average weight over the estimating sample. This reconstitution is close to the estimated effects, though not exactly identical: this reflects the fact that the estimated shocks are not uniformly distributed over the

estimating sample. The blue line represents an aggregated effect on total CPI, still using a linear combination of effects estimated on fresh products and total excluding fresh products, but using their *end-of-sample* weight in 2018. In this case, the estimated effect on total CPI is lower than in the baseline specification, with a maximum response of 0.2% after two months. Finally, the red line represents the same aggregation of effects, but using the weights of fresh products and total excluding fresh products as measured at the *beginning-of-sample* in 1999: in this case, the effect is much stronger than in the baseline, reaching up to 0.7% after two months.

Figure 11. Baseline and alternative effects on CPI inflation

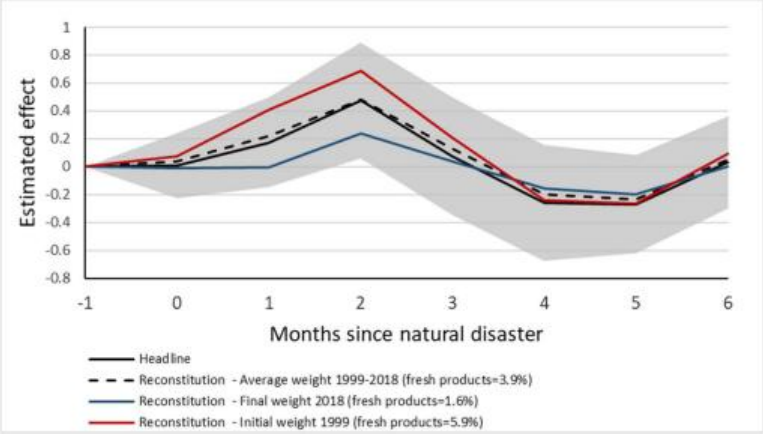

Note: Comparison of the baseline IV estimation of total CPI (solid black line) with a reconstitution of the effect using a linear combination of estimated effects on fresh products and total excluding fresh products with average weights between 1999 and 2018 (dark dotted line), weights as of 1999 (red line) and weights as of 2018 (blue line). Treatment effects are expressed in percent.

7. Conclusion

This paper estimates the sectoral effects on prices of weather-related natural disasters in the four French overseas territories between 1999 and 2018. It thereby contributes to a better understanding of the inflationary impact of physical risks that are likely to increase in the future because of climate change. We find a small positive and transitory effect on total consumer prices after two months (+0.5%). The granularity of the data, which are split into 12 product categories with available weights according to the respective expenditure shares, allows for a full decomposition of the total effect. The response of inflation to weather-related disasters is heterogeneous across CPI components both in terms of timing and amplitude, with a quick and positive response of food inflation (especially fresh food), which is partly offset by a negative contribution of inflation in services and manufactured products. We provide complementary evidence on real activity. Significant reductions in employment in the agricultural and

construction sector provide a plausible narrative for the transmission channels at play, separating between dominant supply versus demand forces. While lower employment in the agricultural sector points toward dominant supply effects in the price response of fresh food, lower demand for housing-related goods and services in conjunction with lower employment in the construction sector are likely to contribute to the negative price response of services and manufactured goods.

Two interesting related findings are worth highlighting. First, we document and quantify the consequences of weather-induced natural disasters for inflation inequality. The distributional effects depend primarily on the differing weight of fresh food in the consumption basket of households, which decreases along the income distribution. Second, we document and quantify how the introduction of price regulation in 2012 affects price-gouging behavior. While the immediate impact is significantly lower after the introduction of a *Bouclier Qualité-Prix*, price responses a few months after the disaster shock are higher, leading to a similar total effect after six months. This result is interesting for policymakers during times of high inflation, in which price regulation is actively discussed again in academia and among policy circles (Neely 2022).

Finally, the paper makes a methodological contribution of interest for follow-up empirical work. Namely, it proposes an IV approach to overcome the measurement problems related to economic damage resulting from physical disaster risk. Instrumenting disaster occurrence in administrative databases with meteorological data leads to comparable results as the direct specification damage functions. Relatedly, the findings underline the importance of a careful modeling of regional seasonality, as inflation and weather-induced disaster might share common seasonality patterns that potentially bias the estimator.

References

Auffhammer, Maximilian (2018). "Quantifying economic damages from climate change", *Journal of Economic Perspectives*, 32(4), 33-52.

Bao, Xiaojia, Puyang Sun, and Jianan Li (2023). "The impacts of tropical storms on food prices: Evidence from China." *American Journal of Agricultural Economics,* 105(2), 576-596.

Baugh, K., Elvidge, C. D., Ghosh, T., and Ziskin, D. (2010). "Development of a 2009 stable lights product using DMSP-OLS data", *Proceedings of the Asia-Pacific Advanced Network*, 30(0), 114.

Beatty, Timothy KM, Gabriel E. Lade, and Jay Shimshack (2021). "Hurricanes and gasoline price gouging." *Journal of the Association of Environmental and Resource Economists,*8(2), 347-374.

Berthier Jean-Pierre, Jean-Louis Lhéritier and Gérald Petit (2010). "Comparaison des prix entre les DOM et la métropole en 2010", *Insee première*, Juillet 2010, n°1304. - 4 p.

Bertinelli, Luisito, and Eric Strobl (2013). "Quantifying the Local Economic Growth Impact of Hurricane Strikes: An Analysis from Outer Space for the Caribbean." *Journal of Applied Meteorology and Climatology*, 52(8), 1688–97.

Cabral, Luis, and Lei Xu (2021). "Seller reputation and price gouging: Evidence from the COVID-19 pandemic." *Economic Inquiry,* 59(3), 867-879.

Cantelmo, Alessandro, Giovanni Melina, and Chris Papageorgiou (2023). "Macroeconomic outcomes in disaster-prone countries." *Journal of Development Economics,* 161(2023), 103037.

Cassar, Alessandra, Andrew Healy, and Carl Von Kessler (2017). "Trust, risk, and time preferences after a natural disaster: experimental evidence from Thailand." *World Development,* 94(2017): 90-105.

Cavallo, Alberto, Eduardo Cavallo and Roberto Rigobon (2014). "Prices and Supply Disruptions during Natural Disasters," *Review of Income and Wealth, International Association for Research in Income and Wealth*, 60(S2), 449-471.

Chen, Xi and William D. Nordhaus (2019). „VIIRS nighttime lights in the estimation of cross-sectional and time-series GDP, *Remote Sensing*, 11(9), 1057.

Ciccarelli, Matteo, Friderike Kuik, and Catalina Martínez Hernández (2023). "The asymmetric effects of weather shocks on euro area inflation." ECB Working Paper, 2798.

Culpepper, Dreda, and Walter Block (2008). "Price gouging in the Katrina aftermath: free markets at work." *International Journal of Social Economics,* 35(7), 512-520.

De Chaisemartin, Clément and Xavier d'Haultfoeuille (2020). "Two-way fixed effects estimators with heterogeneous treatment effects." *American Economic Review,*110(9), 2964-96.

Dell, Melissa, Benjamin F. Jones and Benjamin A. Olken (2012). "Temperature shocks and economic growth: Evidence from the last half century", *American Economic Journal: Macroeconomics*, 4(3), 66-95.

Doyle, Lisa, and Ilan Noy (2015). "The short-run nationwide macroeconomic effects of the Canterbury earthquakes." *New Zealand Economic Papers,* 49(2), 134-156.

Emanuel, Kerry (2011). "Global Warming Effects on U.S. Hurricane Damage" *Weather, Climate, and Society*, 3(4), 261–268.

Faccia, Donata, Miles Parker, and Livio Stracca (2021). "Feeling the heat: extreme temperatures and price stability", ECB Working Paper, 2626.

Felbermayr Gabriel and Jasmin Gröschl (2014). "Naturally negative: the growth effects of natural disasters", *Journal of Development Economics,* 111(2014), 92-106.

Gagnon, Etienne and David López-Salido (2020). "Small Price Responses to Large Demand Shocks," *Journal of the European Economic Association*, 18(2), 792-828.

Gautier, Erwan, Magali Marx and Paul Vertier (2023). "How do Gasoline Prices Respond to a Cost Shock?" *Journal of Political Economy Macroeconomics*.

Grislain-Letrémy, Céline (2018). "Natural Disasters: Exposure and Underinsurance," *Annals of Economics and Statistics*, GENES, issue 129, 53-83.

Hansen, Lars Peter (2022). "Central banking challenges posed by uncertain climate change and natural disasters", *Journal of Monetary Economics*, 125(2022), 1-15.

Heinen, Andréas, Jeetendra Khadan and Eric Strobl (2018). "The Price Impact of Extreme Weather in Developing Countries," *Economic Journal*, 129(619), 1327-1342.

Henderson, J. Vernon, Adam Storeygard, and David N. Weil (2012). "Measuring economic growth from outer space", *American Economic Review*, 102(2), 994-1028.

Hobijn, Bart and David Lagakos (2005). "Inflation Inequality in the United States", *Review of Income and Wealth,* 51(4), 581-606.

Hobijn, Bart, Kristin Mayer, Carter Stennis and Giorgio Topa (2009). "Household Inflation Experiences in the U.S.: A Comprehensive Approach", Federal Reserve Bank of San Francisco Working Paper, 2009-19.

Hugounenq Réjane and Valérie Chauvin (2006) "Les évolutions comparées des prix à la consommation dans les DOM et en métropole". *Bulletin de la Banque de France*, n°151. 33-46.

Jordà, Òscar. (2005). "Estimation and Inference of Impulse Responses by Local Projections." *American Economic Review*, 95(1), 161-182.

Kabundi, Alain, Montfort Mlachila, and Jiaxiong Yao (2022). "How Persistent Are Climate-Related Price Shocks? Implications for Monetary Policy." IMF Working Paper.

Kahn, Matthew E. (2005). "The Death Toll from Natural Disasters: The Role of Income, Geography, and Institutions," *The Review of Economics and Statistics*, 87(2), 271-284.

Kirchberger, Martina (2017). "Natural disasters and labor markets." *Journal of Development Economics,* 125 (2017), 40-58.

Kolstad, Charles D. and Frances C. Moore (2020). "Estimating the economic impacts of climate change using weather observations", *Review of Environmental Economics and Policy*, 14(1).

Kotz, Maximilian, Friderike Kuik, Eliza Lis and Christiane Nickel (2024). "Global warming and heat extremes to enhance inflationary pressures". *Communications Earth & Environment*, 5(116).

Montiel Olea, José Luis, and Mikkel Plagborg-Møller. (2021). "Local projection inference is simpler and more robust than you think." *Econometrica,* 89(4), 1789-1823.

Neely, Christopher J. (2022). "Why price controls should stay in the history books", *The Regional Economist*, Federal Reserve Bank of St. Louis, March 2022.

Neilson, Henry (2009). "Price gouging versus price reduction in retail gasoline markets during Hurricane Rita." *Economics Letters*, 105(1), 11-13.

Noy, Ilan (2009). "The macroeconomic consequences of disasters", *Journal of Development Economics*, 88(2009), 221-231.

Parker, Miles (2018). "The impact of disasters on inflation". *Economics of Disasters and Climate Change*, *2*(1), 21-48.

Pérez-Sindín, Xaquín S. and Tzu-Hsin K. Chen and Alexander V. Prishchepov (2021). "Are night-time lights a good proxy of economic activity in rural areas in middle and low-income countries? Examining the empirical evidence from Colombia", *Remote Sensing Applications: Society and Environment*, 24(2021), 100647.

Schnabel, Isabel (2021). "A new strategy for a changing world", Speech delivered at the virtual Financial Statements series hosted by the Peterson Institute for International Economics, 14 July 2021.

Schumacher, Ingmar and Eric Strobl (2011). "Economic development and losses due to natural disasters: The role of hazard exposure", *Ecological Economics*, 72, issue C, 97-105.

Stock, James H. and Mark W. Watson (2018). "Identification and estimation of dynamic causal effects in macroeconomics using external instruments", *Economic Journal*, 128(610), 917-948.

Strobl, Eric (2011). "The economic growth impact of hurricanes: Evidence from U.S. coastal counties", *Review of Economics and Statistics*, 93(2), 575-589.

Strobl, Eric (2012). "The economic growth impact of natural disasters in developing countries: Evidence from hurricane strikes in the Central American and Caribbean regions", *Journal of Development Economics*, 97(2012), 130-141.

ONLINE APPENDIX

Decomposing the Inflation Response to Weather-Related Disasters

Appendix A. Data

A.1 Consumer prices in French DROMs

Table A.1 – Descriptive statistics of inflation data

	Guadeloupe		French Guiana		Réunion		Martinique		DROMs		France	
Component	m-o-m	sd	m-o-m	sd	m-o-m	sd	m-o-m	sd	m-o-m	sd	m-o-m	sd
Headline	0.12	0.47	0.11	0.31	0.12	0.60	0.12	0.36	0.12	0.43	0.12	0.31
Fresh products	0.22	3.45	0.30	3.41	0.71	9.21	0.26	2.92	0.37	4.75	0.25	3.49
Other food	0.15	0.47	0.12	0.30	0.16	0.38	0.15	0.37	0.14	0.38	0.12	0.21
Tobacco	0.77	2.81	0.67	3.00	0.73	3.90	0.77	2.82	0.73	3.14	0.49	1.72
Manufactured products	0.04	0.93	-0.03	0.26	0.04	0.89	0.02	0.66	0.02	0.68	0.01	1.04
Energy	0.21	1.94	0.24	2.12	0.22	1.81	0.23	1.91	0.22	1.94	0.30	1.66
Services	0.13	0.59	0.14	0.50	0.13	0.80	0.13	0.46	0.13	0.59	0.15	0.41

Note: Moments computed from the first-difference in the logarithm of monthly price indices over the 1999m01 to 2018m04 period. DROMs refers to the unweighted average across all four regions.

Table A.2 – Correlations between main CPI in DROMs and in France (1999m01-2018m04)

Component	**Guadeloupe**	**French Guiana**	**Réunion**	**Martinique**	**DROMs**
Headline	0.22 [0.001]	0.12 [0.06]	-0.04 [0.51]	0.12 [0.06]	0.14 [0.04]
Fresh products	0.05 [0.46]	0.02 [0.76]	0.02 [0.76]	-0.12 [0.06]	0.00 [0.95]
Other food	0.09 [0.18]	0.21 [0.00]	0.37 [0.00]	0.27 [0.00]	0.36 [0.00]
Tobacco	0.25 [0.00]	0.10 [0.13]	0.28 [0.00]	0.14 [0.00]	0.34 [0.00]
Manufactured products	0.31 [0.00]	0.38 [0.00]	-0.21 [0.00]	0.36 [0.00]	0.23 [0.00]
Energy	0.31 [0.00]	0.27 [0.00]	0.21 [0.00]	0.37 [0.00]	0.35 [0.00]
Services	0.41 [0.00]	0.59 [0.00]	0.58 [0.00]	0.44 [0.00]	0.70 [0.00]

Note: p-values in parentheses.

Headline CPI is significantly correlated between overseas regions and France with an average correlation of 0.14, except for Réunion. On average, the correlation is strong and positive for services (0.7) but smaller for manufactured products and energy (0.2 to 0.3), and this holds true for all overseas regions except for Réunion in which the CPI of manufactured products is negatively correlated with that of France. While the CPI of other food products and tobacco is positively correlated between overseas regions and France, this is not the case for the CPI of fresh food products, which is not correlated between overseas regions and France (0.00 on average).

Table A.3 – Coverage ratio of local production

	Fruit		Vegetables	
	Fresh	**All**	**Fresh**	**All**
Guadeloupe	44%	16%	55%	43%
Martinique	31%	13%	39%	26%
French Guiana	94%	79%	90%	81%
Réunion	62%	34%	68%	48%

***Note*:** The table shows the coverage ratio of local production for fruit and vegetables in the four DROMs, both for fresh products (Fresh) and the sum of fresh and non-fresh products (All).
Source: *Observatoire des économies agricoles ultramarines* (2021) – *La couverture des besoins alimentaires dans les DCOM.*

Table A.4 – Composition of CPI aggregates

Fresh food	01131	Fresh or chilled fish
	+ 01133	Fresh or chilled seafood
	+ 01161	Fresh or chilled fruit
	+ 01171	Fresh or chilled vegetables other than potatoes and other tubers
	+ 011741	Fresh or conserved potatoes
Other food	0111	Bread and cereals
	+ 0112	Meat
	+ 01132	Frozen fish
	+ 01134	Frozen seafood
	+ 01135	Dried, smoked or salted fish and seafood
	+ 01136	Other preserved or processed fish and seafood-based preparations
	+ 0114	Milk, cheese and eggs
	+ 0115	Oils and fats
	+ 01162	Frozen fruit
	+ 01163	Dried fruit and nuts
	+ 01164	Preserved fruit and fruit-based products
	+ 01172	Frozen vegetables other than potatoes and other tubers
	+ 01173	Dried vegetables, other preserved or processed vegetables
	+ 011742	Processed potatoes (excluding crisps)
	+ 01175	Crisps
	+ 01176	Other tubers and products of tuber vegetables
	+ 0118	Sugar, jam, honey, chocolate and confectionery
	+ 0119	Food products n.e.c.
	+ 012	Non-alcoholic beverages
	+ 021	Alcoholic beverages
Footwear and garments	0311	Clothing materials
	+ 0312	Garments
	+ 0313	Other articles of clothing and clothing accessories
	+ 0321	Shoes and other footwear
Pharmaceutical products	0611	Pharmaceutical products
	+ 06131	Corrective eye-glasses and contact lenses
	+ 06132	Hearing aids
	+ 06139	Other therapeutic appliances and equipment
Other manufactured products	0431	Materials for the maintenance and repair of the dwelling
	+ 0511	Furniture and furnishings
	+ 05121	Carpets and rugs
	+ 05122	Other floor coverings
	+ 05201	Furnishing fabrics and curtains
	+ 05202	Bed linen
	+ 05203	Table linen and bathroom linen
	+ 05209	Other household textiles
	+ 0531	Major household appliances whether electric or not
	+ 0532	Coffee machines, tea makers and similar appliances
	+ 054	Glassware, tableware and household ustensils
	+ 05511	Motorised major tools and equipment
	+ 05521	Non-motorised small tools
	+ 05522	Miscellaneous small tool accessories
	+ 0561	Non-durable household goods
	+ 0612	Other medical products
	+ 071	Purchase of vehicles
	+ 0721	Spare parts and accessories for personal transport equipment
	+ 07224	Lubricants

	+ 08201	Fixed telephone equipment
	+ 08202	Mobile telephone equipment
	+ 08203	Other equipment of telephone and telefax equipment
	+ 0911	Equipment for the reception, recording and reproduction of sound and picture
	+ 0912	Photographic and cinematographic equipment and optical instruments
	+ 0913	Information processing equipment
	+ 0914	Recording media
	+ 0921	Major durables for outdoor recreation
	+ 0922	Musical instruments and major durables for indoor recreation
	+ 0931	Games, toys and hobbies
	+ 09321	Equipment for sport
	+ 09322	Equipment for camping and open-air recreation
	+ 0933	Gardens, plants and flowers
	+ 093421	Products for pets
	+ 095	Newspapers, books and stationery
	+ 121211	Electric appliances for personal care
	+ 1213	Other appliances, articles and products for personal care
	+ 123111	Jewellery
	+ 123121	Clocks and watches
	+ 123211	Travel goods
	+ 123221	Articles for babies
	+ 123291	Other personal effects n.e.c.
Energy	0451	Electricity
	+ 0452	Gas
	+ 0453	Liquid fuels
	+ 0454	Solid fuels
	+ 07221	Diesel
	+ 07222	Petrol
	+ 07223	Other fuels for personal transport equipment
Petroleum products	04522	Liquefied hydrocarbons (butane, propane, etc.)
	+ 0453	Liquid fuels
	+ 07221	Diesel
	+ 07222	Petrol
	+ 07223	Other fuels for personal transport equipment
Rents	0411	Actual rentals paid by tenants
	+ 0441	Water supply
	+ 0442	Refuse collection
	+ 0443	Sewage collection
	+ 0455	Heat energy
	+ 05204	Repair of household textiles
	+ 05523	Repair of non-motorised small tools and miscellaneous accessories
Health services	062	Out-patient services
Transportation services	0731	Passenger transport by railway
	+ 0732	Passenger transport by road
	+ 0733	Passenger transport by air
	+ 0734	Passenger transport by sea and inland waterway
	+ 0735	Combined passenger transport
Communication services	081	Postal services
	+ 083	Telephone and telefax services
Other services	0314	Cleaning, repair and hire of clothing
	+ 032201	Repair and hire of footwear
	+ 0432	Services for the maintenance and repair of the dwelling
	+ 0444	Other services relating to the dwelling n.e.c.

	+ 05123	Services of laying of fitted carpets and floor coverings
	+ 0513	Repair of furniture, furnishings and floor coverings
	+ 05204	Repair of household textiles
	+ 0533	Repair of household appliances
	+ 05404	Repair of glassware, tableware and household utensils
	+ 05512	Repair, leasing and rental of major tools and equipment
	+ 05523	Repair of non-motorised small tools and miscellaneous accessories
	+ 0562	Cleaning services
	+ 0723	Maintenance and repair of personal transport equipment
	+ 0724	Other services in respect of personal transport equipment
	+ 0736	Other purchased transport services
	+ 08204	Repair of telephone or telefax equipment
	+ 0915	Repair of audiovisual, photographic and information processing equipment
	+ 0923	Maintenance and repair of other major durables for recreation and culture
	+ 09323	Repair of equipment for sport, camping and open-air recreation
	+ 09341	Purchase of pets
	+ 0935	Veterinary and other services for pets
	+ 094	Recreational and cultural services
	+ 096	Package holidays
	+ 10	Education
	+ 11	Restaurants and hotels
	+ 1211	Hairdressing salons and personal grooming establishments
	+ 121221	Repair of electric appliances for personal care
	+ 123131	Repair of jewellery, clocks and watches
	+ 123231	Repair of other personal effects
	+ 124	Social protection
	+ 125	Insurance
	+ 126	Financial services n.e.c.
	+ 127	Other services n.e.c.

Figure A.1. Seasonal variations of monthly CPI inflation in DROMs

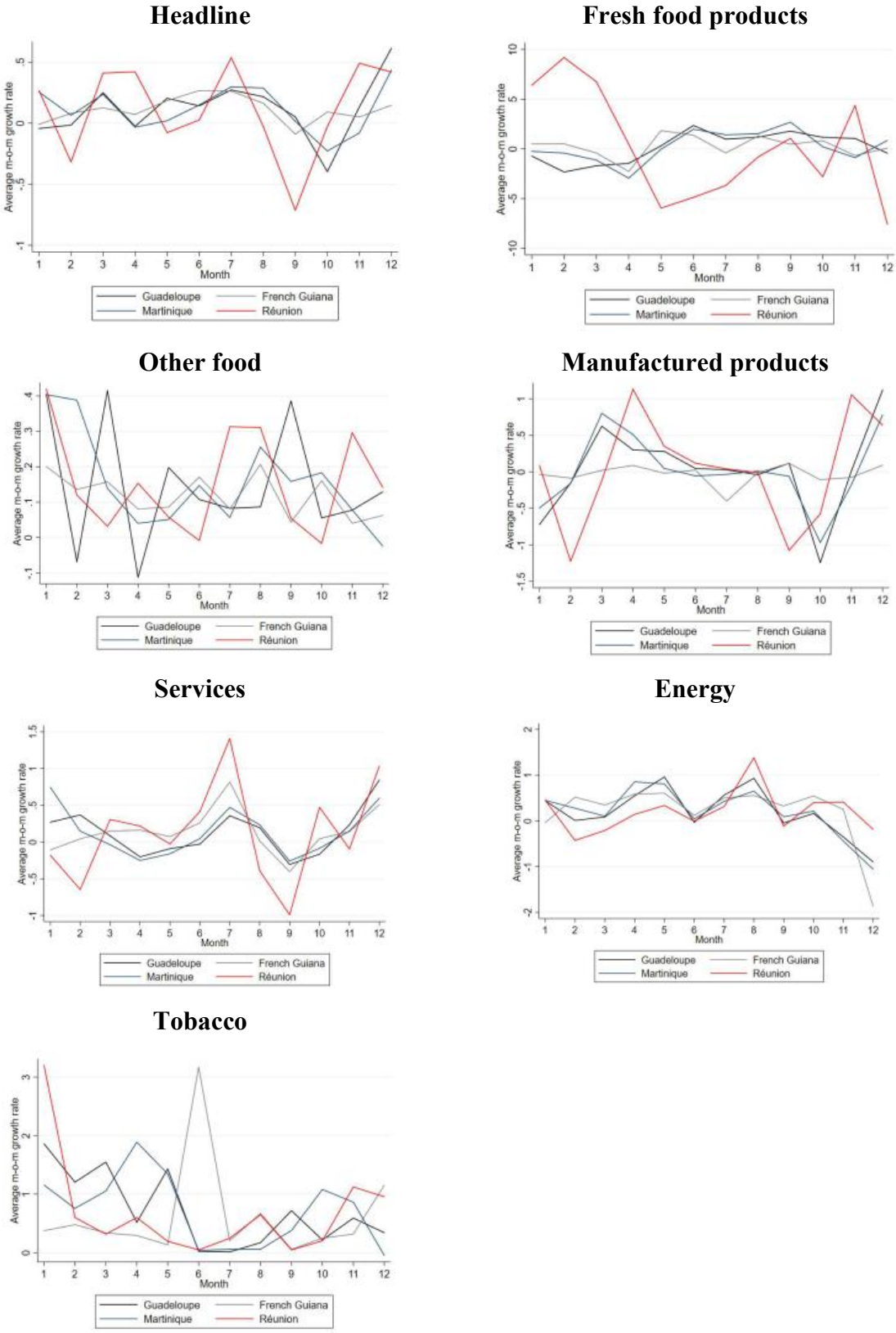

Note: Average monthly variation (in %) of CPI for each component.

A.2 Composition of consumer baskets across overseas regions

The composition of consumer baskets is heterogeneous across French territories and varies over time. Table A.5 reports the weights of each aggregate according to the French statistical office (INSEE) over our sample period, in each region, and the unweighted mean over the sample. Food including tobacco represents about 18% of the consumer basket in the considered region at the end of the sample, with a weight that is declining over time. Fresh products represent roughly 10% of the food basket in 2018 (1.6% of the CPI basket), and its weight strongly decreased over time from 5.9% in 1999. Services represent about 45% of the consumer basket at the end of the sample, with a maximum weight of 47% in Réunion and a minimum weight of 43% in Guadeloupe. Contrary to food, the weight of services increases over time in all territories. The main component is other services (see Table A.4 for details about the composition of this aggregate), which represents about 22% of the total basket in 2019, and whose weight increased over time. Manufactured products represent 29.9% of the CPI basket in 2019, only slightly above the sample mean.

Table A.5 – Weight of the main aggregates of Consumer Price Index

	Guadeloupe		**French Guiana**		**Réunion**		**Martinique**		**DROMs**		**France**	
Aggregate	**Weight 2018**	**Weight 1999-2018**	**Weight 2018**	**Weight 1999-2018**	**Weight 2018**	**Weight 1999-2018**	**Weigh 2018**	**Weight 1999-2018**	**Weight 2018**	**Weight 1999-2018**	**Weight 2018**	**Weight 1999-2018**
Food	1,709	2,226	1,757	2359	1,812	2181	1,897	2,140	1,794	2,226	1,820**	1,849**
Fresh products	179	453	162	402	121	263	180	463	160	395	243	218
Other food	1,441	1,698	1434	1847	1,523	1748	1,601	1,623	1,500	1,729	1,384	1,460
Tobacco	89	75	161	110	168	172	116	55	133	103	193	193
Manufactured products	3,344	3,025	2,930	2535	2,748	3058	2,871	2,850	2,973	2,867	2,594	2,949
Footwear and garment	482	626	663	616	506	641	483	676	533	640	416	477
Other manuf. products	2,290	2,101	1,850	1705	1,932	2208	1,924	1,925	1,999	1,985	1,753	2,029
Pharmaceutical products	572	298	417	214	360	209	464	249	453	242	425	443
Energy	694	903	789	733	642	748	791	858	729	810	777	776
Petroleum products	498	691	572	507	464	532	592	645	531	594	408	454
Services	4,253	3,847	4,524	4372	4,748	4013	4,441	4,152	4,491	4,096	4,809	4,404
Transportation*	223	428	304	440	256	426	163	236	236	382	282	246
Communication*	409	287	390	387	374	445	425	351	399	367	223	257
Health	714	367	566	236	968	387	657	348	726	334	617	534
Rents	774	820	1,239	1618	907	988	904	1,014	956	1,110	764	750
Other services	2,132	2063	2025	1878	2,243	1970	2,292	2,258	2,173	2,042	2,923	2,617

* Data only available since 2010 for all DROMs.

***Note*:** The table shows the weight of the main components of CPI in the four DROMs, and in France, for 2018 and for the 1999-2018 period. The average for the four DROMs is an unweighted mean.

Comparing the weights in overseas regions to those in metropolitan France, three facts stand out. First, the weight structure is more stable over time in metropolitan France. Second, the weights in overseas regions and in France differ mainly with respect to food excluding fresh products (which is higher in DROMs) and service (which is lower in DROMs). Thirdly, the composition of consumption baskets in overseas regions are converging to the composition measured in metropolitan France.

A.3 Real activity

2.1.2 Data on economic activity

Table A.6 – Descriptive statistics on real activity

	Guadeloupe	French Guiana	Réunion	Martinique	DROMs
Employment (share in total, in %)*					
Agriculture (AZ)	1.48	0.74	1.12	3.75	1.77
Food manufacturing (C1)	2.47	1.13	2.58	2.20	2.09
Extractive industry (C2)	1.83	2.77	1.47	2.14	2.05
Manufacturing – machines (C3)	0.19	0.16	0.29	0.17	0.20
Manufacturing – transports (C4)	0.02	0.27	0.04	0.02	0.09
Manufacturing – other (C5)	2.62	3.93	2.62	2.43	2.90
Construction (FZ)	4.88	6.25	5.69	4.94	5.44
Car repair (GZ)	12.64	9.30	13.10	11.47	11.63
Transports (HZ)	4.69	5.12	4.79	4.68	4.82
Accommodation – restaurants (IZ)	3.90	3.40	2.96	4.00	3.56
Information – communication services (JZ)	1.82	1.20	1.65	1.70	1.59
Finance – insurance (KZ)	2.79	1.17	2.32	2.92	2.30
Real estate (LZ)	0.56	0.62	0.79	0.67	0.66
Scientific – administrative (MN)	8.22	6.51	8.23	8.89	7.96
Public administration (OQ)	44.55	51.12	42.35	41.14	44.79
Other services (RU)	6.21	4.33	8.96	7.92	6.85
Interim	1.09	2.13	1.10	1.02	1.34
Number of overnight stays in hotels (thousands)**	90.74	28.81	87.83	102.75	77.53

Note: The table shows average values of real activity variables used in the main analysis, from the beginning of data availability until April 2018. * Data since 2010. ** Data since 2011.

We complement our empirical analysis with some sectoral data on real activity. We include sectoral employment data at quarterly frequency, available since 2010. Employment in overseas regions is dominated by services: non-commercial services (public administration) represent

about 45% of employment, and commercial services represent about 39% of employment. In contrast, the manufacturing industry represents only about 7% of total employment, and the construction sector about 5%, followed by the agricultural sector with 2% (Table A.6).

To assess the effect of natural disasters on the tourism sector, we also include monthly hotel overnight stays in our analysis. They amount to 77,000 on average every month, which roughly corresponds to 15% of the average population of overseas regions.

A.4 Administrative disaster databases

Table A.7 – Overlap between the administrative measures of shocks

		Number (%) in		Number (%) in			
	N	GASPAR	EM-DAT	Guadeloupe	French Guiana	Réunion	Martinique
GASPAR	68	-	11 (16.2%)	21 (30.9%)	5 (7.3%)	22 (32.3%)	20 (29.4%)
EM-DAT	12	11 (91.7%)	-	3 (25%)	0 (0%)	5 (41.7%)	4 (33.3%)
All admin.*	**69**	**-**	**-**	**21 (30.4%)**	**5 (7.2%)**	**23 (33.3%)**	**20 (30%)**

Note: The table shows descriptive statistics on the distribution of natural disasters in four French overseas territories. "All admin" is the union between GASPAR and EM-DAT events.

Table A.8 – Share of total administrative shocks by month of the year

Month	Réunion	Guadeloupe	Martinique	French Guiana
1	26.09	9.52	0	20.00
2	34.78	0	0	0
3	8.70	4.76	0	0
4	21.74	0.00	10.00	20.00
5	4.35	14.29	10.00	60.00
6	0	4.76	0	0
7	0	0	5.00	0
8	0	4.76	10.00	0
9	0	19.05	20.00	0
10	0	14.29	20.00	0
11	0	19.05	15.00	0
12	4.35	9.52	10.00	0

Note: The table shows the share of total number of administrative shocks occurring during each calendar month, in the different DROMs. 34.78% of all shocks in Réunion occurred during the month of February.

A.5 Meteorological data

Figure A.2. Location of weather stations

a) Réunion

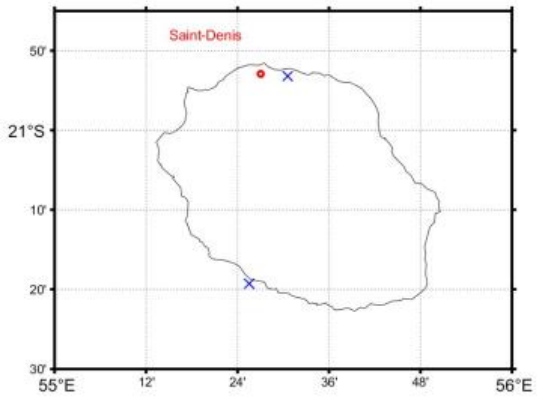

b) French Guiana

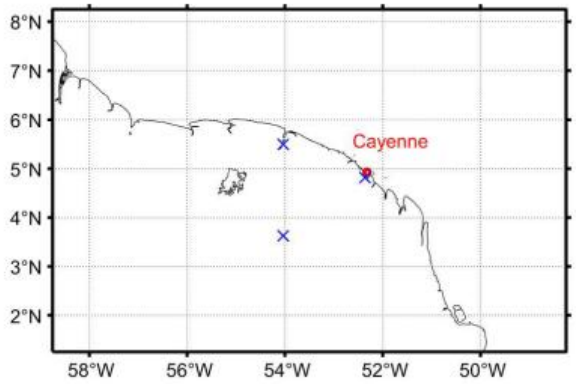

c) Guadeloupe

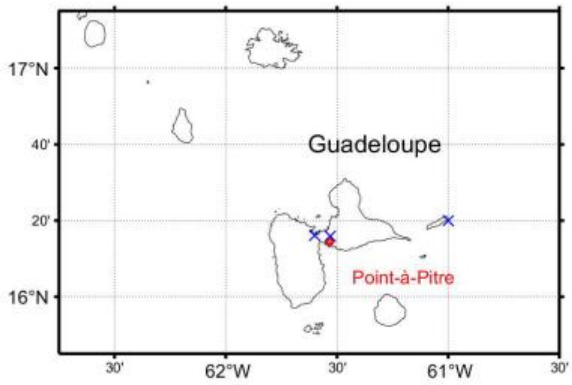

d) Martinique

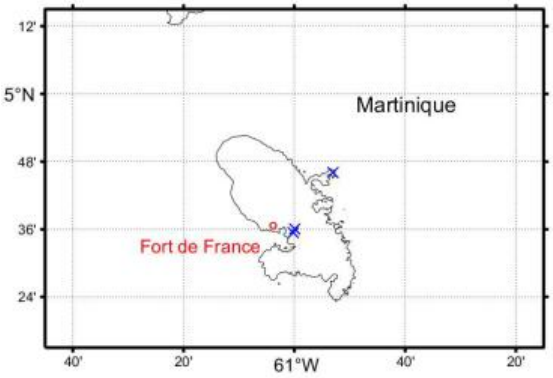

Note: Weather stations from the Global Surface Summary of the Day (GSOD) database in Réunion (St Denis Gillot, St Pierre Pierrefonds), Martinique (La Lamentin, Martinique Aime Césaire International Airport, Trinité Caravelle), Guadeloupe (La Desirade, Le Raizet, Point-à-Pitre International Airport), and French Guiana (Maripasoula, Rochambeau, St Laurent du Maron).

Figure A.3. Wind speed via remote sensing

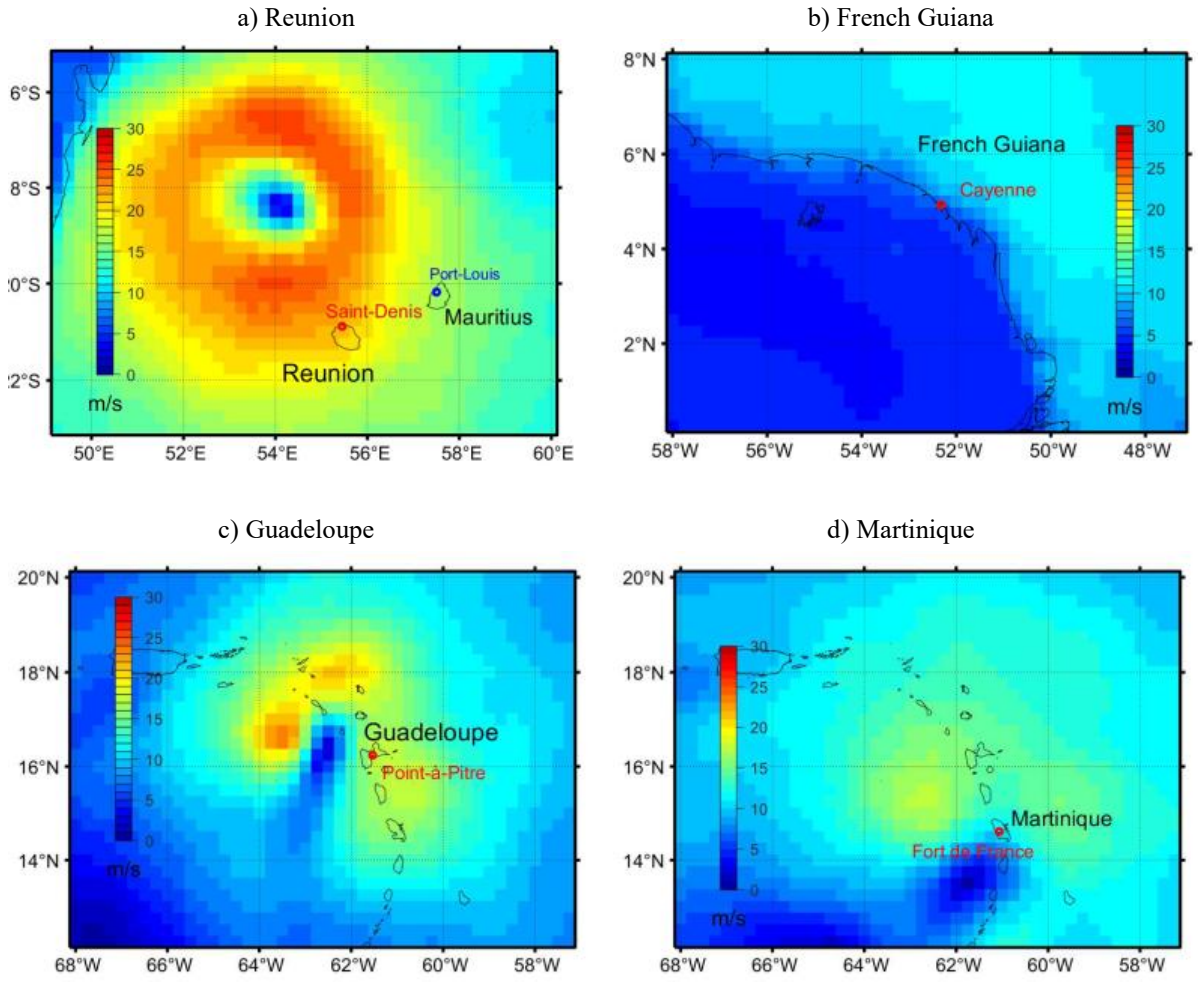

Note: Wind speed via remote sensing from the Cross-Calibrated Multi-Platform (CCMP), measured on a 0.25-degree grid in meters per second on a scale between zero and 30. Panels a to d show the maximum six-hour average wind speed, which amount to 27.76 m/s 2007-Feb-25 (12AM) in Réunion (cyclone Gamede), 17.26 m/s 17-Aug-2007 (6PM) in Martinique (hurricane Dean), 21.52 m/s 19-Sep-2017 (6PM) in Guadeloupe (hurricane Maria), and 13.52 m/s 10-Mar-2015 (12 PM) in French Guiana.

Figure A.4. Precipitation via remote sensing

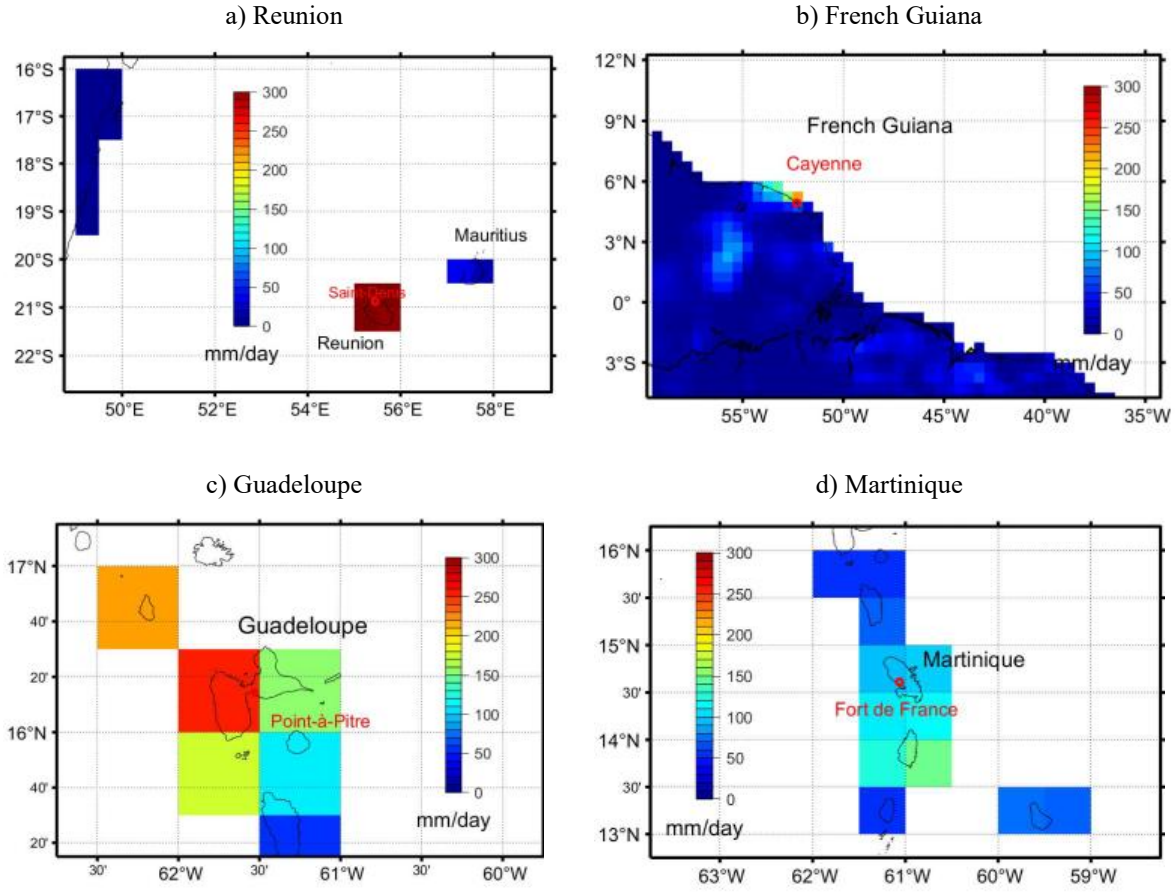

Note: Precipitation via remote sensing from the Climate Prediction Center (CPC), measured on a 0.5-degree grid in millimeters per day. Panels a to d show the maximum daily precipitation, which is 319.11 mm, 29.01.2011 in Réunion, 141.06 mm, 28.09.2016 in Martinique, 252.59 mm, 19.11.1999 in Guadeloupe, and 212.79 mm, 08.04.2000 in French Guiana.

Table A.9 – Summary statistics of meteorological data

	Precipitation				Wind speed			
	Remote sensing (CPC)		Weather stations (GSOD)		Remote sensing (CCMP)		Weather stations (GSOD)	
	Mean	SD	Mean	SD	Mean	SD	Mean	SD
Réunion	43.25	45.92	110.08	122.48	13.12	2.55	2.75	0.46
French Guiana	69.82	30.97	142.67	86.21	10.06	1.31	1.62	0.35
Guadeloupe	36.67	25.10	89.03	92.81	11.61	1.58	1.99	0.58
Martinique	40.36	23.98	97.32	79.19	11.17	1.26	2.45	0.70
Unweighted average	47.53	31.49	109.78	95.17	11.49	1.68	2.20	0.52

Note: All data was harmonized for comparability. Precipitation is measured in cumulative millimeters per day (conversion: 0.01 inches = 0.254 mm). Wind speed is measured in meters/second (conversion: 0.1 knots = 0.0514444 m/s).

Table A.10 – Météo-France events

Region	Date	Event name	Event type
Réunion	24-Feb-2007	Gamede	cyclone
Réunion	3-Mar-2006	Diwa	cyclone
Réunion	21-Jan-2002	Dina	cyclone
Réunion	3-Jan-2018	Ava	cyclone
Réunion	9-Mar-1999	Davina	cyclone
Réunion	4-Mar-2018	Dumazile	cyclone
Réunion	1-Jan-2014	Bejisa	cyclone
Réunion	7-Mar-2015	Haliba	cyclone
French Guiana	15-May-2013	-	extreme rain
French Guiana	24-Jan-2010	-	extreme rain
French Guiana	1-Jun-2008	-	extreme rain
French Guiana	8-May-2006	-	extreme rain
French Guiana	30-Apr-2000	-	extreme rain
French Guiana	17-May-2000	-	extreme rain
Guadeloupe	10-Nov-2018	-	extreme rain
Guadeloupe	18-Sep-2017	Maria	hurricane
Guadeloupe	12-Oct-2012	Rafael	hurricane
Guadeloupe	3-Jan-2011	-	extreme rain
Guadeloupe	30-Aug-2010	Earl	hurricane
Guadeloupe	17-Aug-2007	Dean	hurricane
Guadeloupe	18-Nov-1999	Lenny	hurricane
Guadeloupe	21-Oct-1999	Jose	hurricane
Martinique	16-Apr-2018	-	extreme rain
Martinique	31-Dec-2017	-	extreme rain
Martinique	28-Sep-2016	Matthew	hurricane
Martinique	6-Nov-2015	-	extreme rain
Martinique	12-Oct-2012	Rafael	hurricane
Martinique	1-Aug-2011	Emily	hurricane
Martinique	30-Oct-2010	Tomas	hurricane
Martinique	4-May-2009	-	extreme rain
Martinique	17-Aug-2007	Dean	hurricane
Martinique	18-Nov-1999	Lenny	hurricane

Note : Events obtained from Météo-France websites documenting extreme events in the four regions:
http://pluiesextremes.meteo.fr/lareunion/Le-club-des-500-mm.html,
http://pluiesextremes.meteo.fr/guyane/-Evenements-memorables-.html
http://pluiesextremes.meteo.fr/antilles/-Evenements-memorables-.html

Appendix B. Additional results

Figure B.1. First-stage fitted values: predicted probability of a significant natural disaster

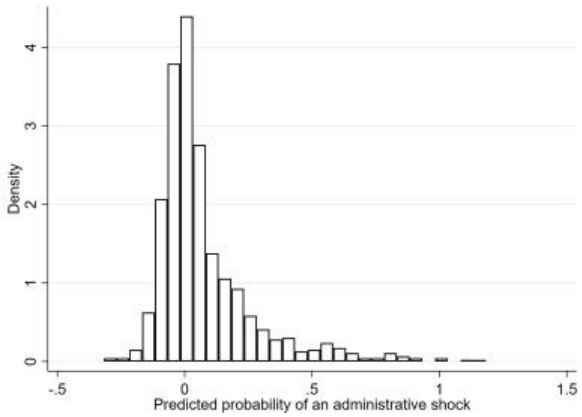

Note: The figure shows the density plot of fitted values $\widehat{\omega}_{it}$ of model (1). Since the dependent variable is an indicator variable associated with natural disaster events with large economic damages, we interpret $\widehat{\omega}_{it}$ as the predicted probability of an economically significant natural disaster as a function of meteorological data.

Figure B.2. First-stage fitted values: predicted probability conditional on the occurrence of GASPAR shocks

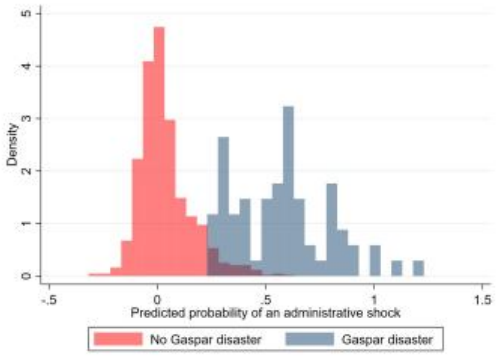

Figure B.3. First-stage fitted values: predicted probability conditional on the occurrence of EM-DAT shocks

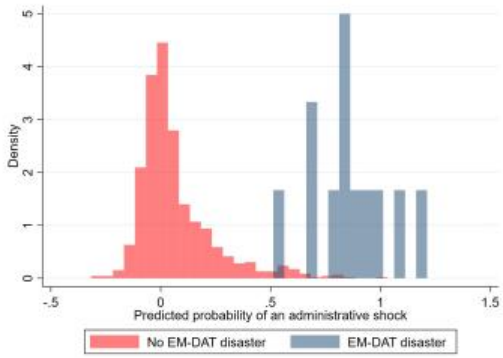

Figure B.4. First-stage fitted values: predicted probability conditional on the occurrence of administrative shocks

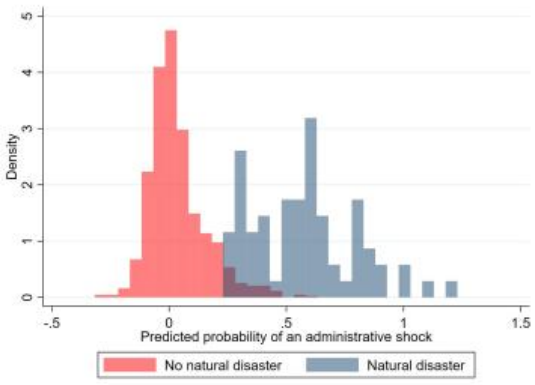

Figure B.5. Main results – CPI components - OLS

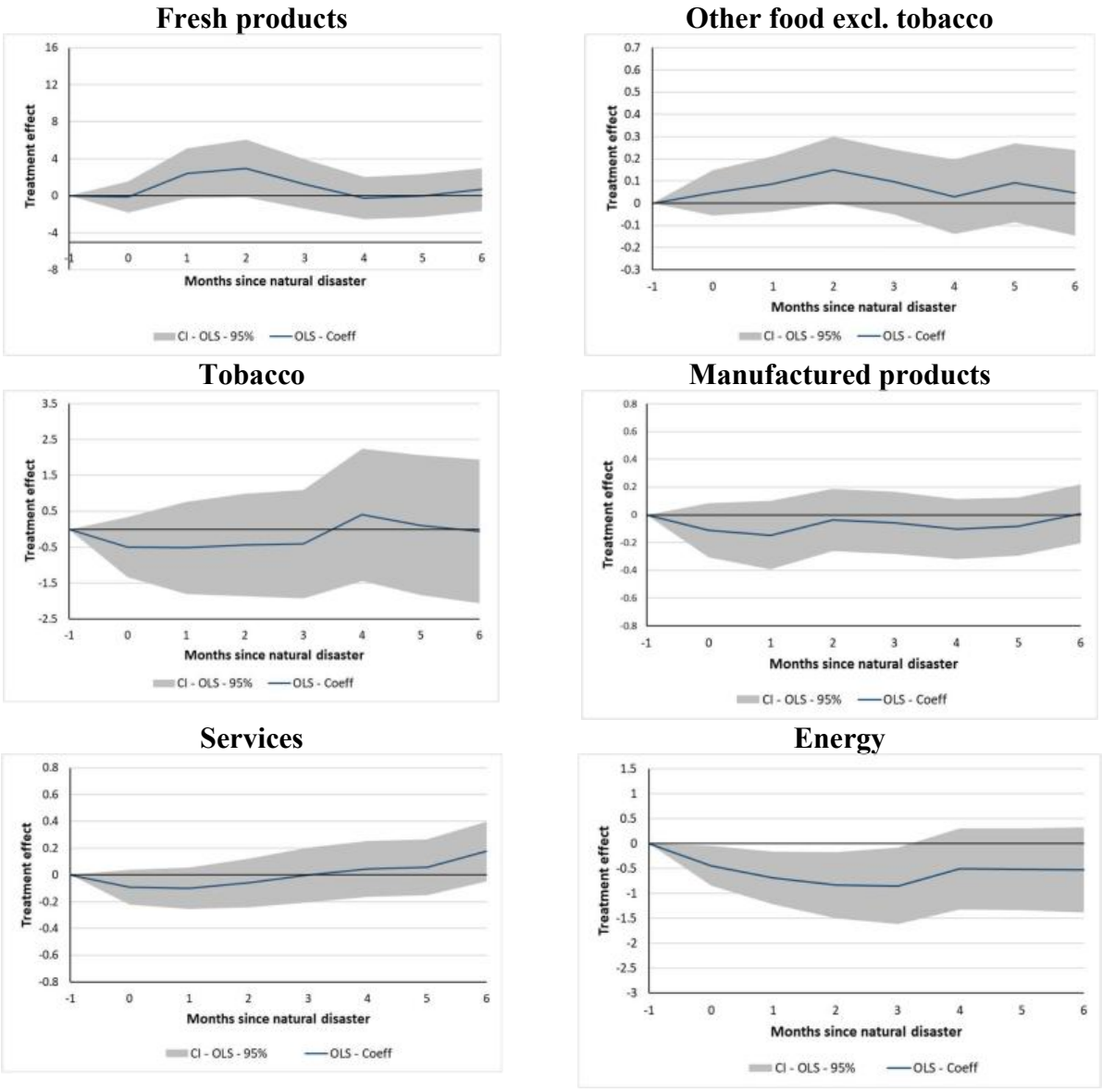

Note: The figures plot the cumulated impulse response function of CPI components in our baseline OLS specification. Treatment effects are expressed in percent. 95% confidence intervals with robust standard errors in the shaded areas.

Table B.1 – Baseline effects on CPI inflation for all available aggregates

	T=0	T=1	T=2	T=3	T=4	T=5	T=6
Food excl. tobacco	0.39	1.62***	2.28***	0.86	-0.38	0.02	0.57
	(0.24)	(0.42)	(0.63)	(0.57)	(0.50)	(0.43)	(0.41)
Other food	0.29***	0.13	0.31***	0.24*	0.03	0.31**	0.16
	(0.10)	(0.12)	(0.12)	(0.14)	(0.14)	(0.15)	(0.17)
Fresh products	1.89	9.48***	10.60***	3.96	-2.11	-1.72	2.03
	1.49	2.29	3.13	2.65	2.32	2.32	2.25
Tobacco	-0.04	-0.38	-0.35	0.00	-0.60	-0.32	-0.38
	(0.48)	(0.75)	(0.90)	(1.04)	(1.26)	(1.46)	(1.51)
Energy	-0.48	-0.20	0.35	-0.04	-0.25	-1.10	-1.17
	(0.53)	(0.54)	(0.58)	(0.67)	(0.74)	(0.78)	(0.82)
Petroleum products	-0.69	-0.35	0.43	-0.13	-0.49	-1.68	-1.74
	(0.73)	(0.75)	(0.79)	(0.92)	(0.99)	(1.04)	(1.08)
Manufactured products	-0.13	-0.27	-0.02	0.11	-0.22	-0.31	-0.15
	(0.18)	(0.23)	(0.21)	(0.19)	(0.20)	(0.19)	(0.24)
Other manuf.	0.00	-0.11	-0.02	-0.04	-0.12	-0.20*	-0.28*
	(0.08)	(0.10)	(0.11)	(0.10)	(0.12)	(0.11)	(0.15)
Footwear and garments	-0.28	-0.95	-0.27	0.87	-0.75	-1.03	0.10
	(0.79)	(0.92)	(0.81)	(0.75)	(0.78)	(0.79)	(0.83)
Pharmaceutical products	-0.07	-0.01	0.02	-0.15	0.00	-0.03	-0.26
	(0.12)	(0.15)	(0.16)	(0.16)	(0.21)	(0.23)	(0.28)
Services	-0.03	-0.19	-0.12	-0.32*	-0.20	-0.25	0.06
	(0.13)	(0.17)	(0.19)	(0.18)	(0.21)	(0.20)	(0.21)
Other services	-0.16	-0.18	-0.12	-0.21	-0.27	-0.45*	-0.22
	(0.16)	(0.18)	(0.21)	(0.22)	(0.25)	(0.26)	(0.27)
Rents	-0.05	-0.20**	0.11	0.07	0.20	0.18	0.33
	(0.07)	(0.10)	(0.15)	(0.17)	(0.20)	(0.21)	(0.23)
Communication services	-0.35**	-0.50	-0.66*	-0.61*	-0.64*	-0.31	0.04
	0.18	0.34	0.38	0.37	0.37	0.36	0.44
Health services	-0.28**	-0.17	-0.20	-0.29	-0.37	-0.27	-0.41
	(0.13)	(0.18)	(0.20)	(0.23)	(0.25)	(0.28)	(0.32)
Transportation services	-0.22	0.27	1.26	0.31	-0.61	3.59	3.74
	(2.02)	(2.04)	(2.05)	(1.93)	(2.57)	(2.42)	(3.47)
Total	0.01	0.17	0.48*	0.08	-0.26	-0.27	0.03
	(0.12)	(0.16)	(0.21)	(0.21)	(0.21)	(0.18)	(0.17)
N	926	926	926	926	926	926	926

***Note*:** Cumulative impulse response functions of consumer prices in the four DROMs estimated between 1999m01 and 2018m04, using 2SLS local projections. Robust standard errors in parentheses.
*p < 0.10; **p < 0.05; *** p < 0.01.

Table B.2 – Main results – CPI components – OLS

	T=0	T=1	T=2	T=3	T=4	T=5	T=6
OLS estimates							
Total	-0.13**	-0.04	0.06	-0.01	-0.02	0.04	0.12
	(0.06)	(0.09)	(0.11)	(0.11)	(0.10)	(0.09)	(0.10)
Fresh products	-0.11	2.41*	2.94*	1.27	-0.25	0.02	0.69
	(0.86)	(1.37)	(1.59)	(1.37)	(1.17)	(1.18)	(1.18)
Other food excl. tobacco	0.05	0.09	0.15*	0.10	0.03	0.09	0.05
	(0.05)	(0.06)	(0.08)	(0.07)	(0.09)	(0.09)	(0.10)
Manufactured products	-0.11	-0.15	-0.04	-0.06	-0.10	-0.08	0.01
	(0.10)	(0.13)	(0.11)	(0.11)	(0.11)	(0.11)	(0.11)
Services	-0.09	-0.10	-0.06	0.00	0.04	0.06	0.18
	(0.07)	(0.08)	(0.09)	(0.10)	(0.11)	(0.11)	(0.11)
Energy	-0.45**	-0.69**	-0.83**	-0.85**	-0.51	-0.51	-0.53
	(0.20)	(0.27)	(0.34)	(0.39)	(0.41)	(0.42)	(0.44)
Tobacco	-0.49	-0.52	-0.43	-0.41	0.40	0.11	-0.05
	(0.43)	(0.66)	(0.73)	(0.77)	(0.94)	(0.99)	(1.02)

***Note*:** Cumulative impulse response functions of consumer prices in the four DROMs estimated between 1999m01 and 2018m04, using OLS local projections. Robust standard errors in parentheses.

*p < 0.10; **p < 0.05; *** p < 0.01.

Table B.3 – Main effects of meteorological extreme events on sectoral employment and on hotel stays (2SLS)

	T=0	T=1	T=2	T=3	T=4	T=5	T=6
Hotel stays							
Overnight hotel stays	-0.23	10.54**	7.88*	7.64	3.52	1.56	-0.21
	(3.59)	(4.66)	(4.52)	(5.07)	(5.78)	(4.99)	(3.82)
Employment							
Total	-0.37*	-0.33	-0.18	-0.16	0.23	0.16	0.13
	(0.21)	(0.27)	(0.28)	(0.36)	(0.37)	(0.39)	(0.39)
Agriculture (AZ)	-1.08	-2.29*	-3.22**	-1.27	-1.55	-1.90	-1.88
	(0.86)	(1.26)	(1.30)	(1.59)	(1.73)	(1.69)	(2.18)
Food manuf. (C1)	-0.03	-0.35	-1.41	0.40	-0.79	-0.91	-1.14
	(0.58)	(0.78)	(0.89)	(1.13)	(1.27)	(1.31)	(1.26)
Extractive industry (C2)	-0.29	0.20	-0.94	-1.02	-1.43	-1.25	-0.40
	(0.37)	(0.70)	(0.78)	(0.86)	(1.06)	(1.02)	(1.39)
Manuf. – machines (C3)	0.46	1.01	-0.10	0.42	0.96	3.52	3.06
	(1.21)	(1.78)	(2.01)	(1.87)	(2.06)	(2.15)	(2.38)
Manuf. – transports (C4)	5.73	1.49	7.29	3.79	-4.57	-8.42	-12.24
	(5.64)	(8.90)	(8.70)	(8.05)	(11.26)	(10.83)	(10.26)
Manuf. – others (C5)	-0.23	-0.05	0.18	-0.04	0.14	0.20	1.20
	(0.27)	(0.46)	(0.51)	(0.62)	(0.68)	(0.77)	(0.80)
Construction (FZ)	-0.72*	-1.06*	-1.38*	-0.80	0.11	0.19	0.23
	(0.41)	(0.62)	(0.75)	(1.02)	(1.23)	(1.27)	(1.44)
Car repair (GZ)	-0.12	-0.39	-0.01	0.49	0.94*	1.16**	1.03*
	(0.27)	(0.35)	(0.44)	(0.44)	(0.50)	(0.56)	(0.58)
Transports (HZ)	-0.28	-0.03	0.17	0.10	0.02	0.64	-0.03
	(0.32)	(0.55)	(0.61)	(0.64)	(0.78)	(0.69)	(0.73)
Accom. – restaurants (IZ)	0.32	0.68	0.36	0.23	0.03	0.25	-0.15
	(0.39)	(0.55)	(0.64)	(0.75)	(0.82)	(0.86)	(0.81)
Info. – comm (JZ)	-1.03*	-0.88	1.04	1.55	1.97	1.20	2.37**
	(0.53)	(0.85)	(1.21)	(1.26)	(1.38)	(1.22)	(1.20)
Finance – insurance (KZ)	0.12	0.47	0.15	0.54	-0.40	0.28	-0.14
	(0.61)	(0.73)	(0.76)	(0.70)	(0.74)	(0.76)	(0.68)
Real estate (LZ)	-0.40	-1.14	-0.87	-0.59	-1.71	-0.91	0.30
	(0.58)	(0.83)	(0.97)	(1.03)	(1.35)	(1.34)	(1.36)
Scientific – admin (MN)	-0.49	-0.11	0.40	0.47	0.37	0.69	0.09
	(0.40)	(0.59)	(0.63)	(0.83)	(0.98)	(1.08)	(1.15)
Public admin (OQ)	-0.44*	-0.35	-0.12	-0.48	0.22	-0.13	0.09
	(0.24)	(0.33)	(0.34)	(0.41)	(0.41)	(0.45)	(0.47)
Other services (RU)	-0.15	-0.21	-0.58	-1.20	-0.73	-1.01	-0.95
	(0.41)	(0.63)	(0.69)	(0.84)	(0.98)	(0.97)	(0.91)
Interim	5.57	9.22	7.02	15.53**	7.97	15.97*	5.89
	(5.46)	(6.85)	(7.10)	(7.26)	(8.17)	(8.40)	(7.86)

***Note*:** Cumulative impulse response functions of real activity data in the four DROMs estimated between 1999m01 and 2018m04, using 2SLS local projections. T-stat with robust standard errors in parentheses.
*p < 0.10; **p < 0.05; *** p < 0.01.

Figure B.6. Comparison of baseline damage functions with wind-only damage functions, at top percentile

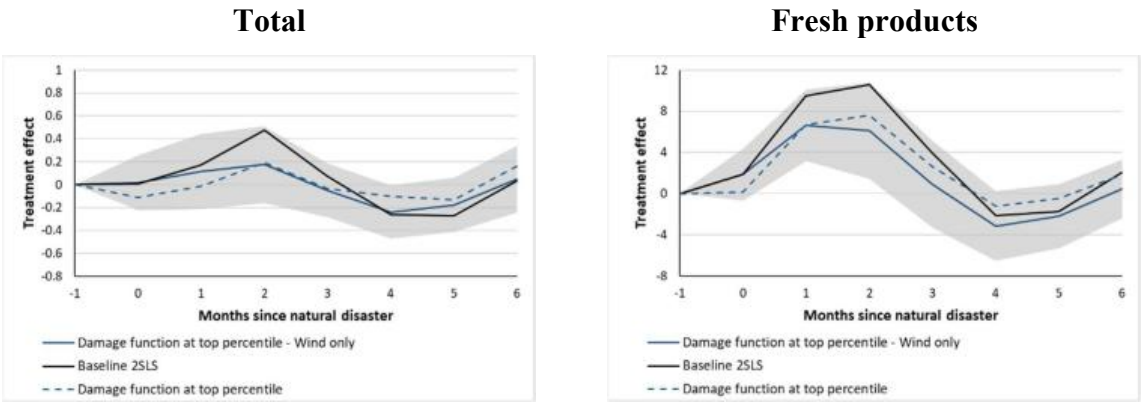

Note: The figures plot the cumulated impulse response function for headline CPI and fresh products CPI, for wind damage function (in solid blue), compared to our baseline 2SLS (in black) and to our combined wind and rain damage function (dotted blue). The damage functions are evaluated at the top percentile of shocks, and shaded areas represent 95% confidence intervals with robust standard errors for wind-only damage functions. Treatment effects are expressed in percent.

Figure B.7. Comparison of baseline damage functions with rain-only and rain-only damage functions, at top percentile

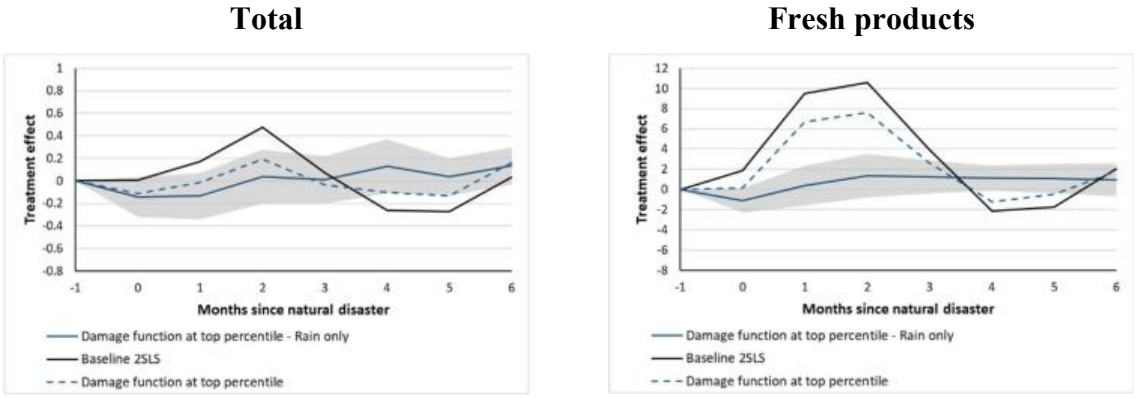

Note: The figures plot the cumulated impulse response function for headline CPI and fresh products CPI, for rain damage function (in solid blue), compared to our baseline 2SLS (in black) and to our combined wind and rain damage function (dotted blue). The damage functions are evaluated at the top percentile of shocks, and shaded areas represent 95% confidence intervals with robust standard errors for rain-only damage functions. Treatment effects are expressed in percent.

Table B.4 – Robustness analysis for other components

	T=0	T=1	T=2	T=3	T=4	T=5	T=6
(A) Other food excl. tobacco							
2SLS - Baseline	0.29***	0.13	0.31***	0.24*	0.03	0.31**	0.16
2SLS – Baseline – no Réunion	0.27**	0.16	0.21	0.20	-0.01	0.40*	0.31
2SLS – Baseline, 3 lags shock	0.24***	0.15	0.33***	0.24*	0.04	0.29**	0.13
2SLS –3 lags CPI	0.24***	0.08	0.26**	0.19	0.01	0.29**	0.14
2SLS – Baseline excl. shock < 6months	0.37***	0.17	0.40**	0.30	0.02	0.39**	0.20
2SLS – 6 lags forward	0.23**	0.18	0.31***	0.28**	0.10	0.29*	0.19
2SLS – Baseline, weather station data	0.23**	0.09	0.26**	0.19	0.02	0.31**	0.21
(B) Manufactured products							
2SLS - Baseline	-0.13	-0.27	-0.02	0.11	-0.22	-0.31	-0.15
2SLS – Baseline – no Réunion	-0.09	0.04	-0.07	-0.11	-0.35	-0.47*	-0.40
2SLS – Baseline, 3 lags shock	-0.16	-0.23	0.05	0.14	-0.08	-0.11	0.08
2SLS –3 lags CPI	-0.17	-0.32*	-0.03	0.04	-0.32*	-0.37**	-0.21
2SLS – Baseline excl. shock < 6months	-0.17	-0.35	-0.03	0.15	-0.29	-0.39	-0.19
2SLS – 6 lags forward	-0.11	-0.35	0.00	0.08	-0.23	-0.29	-0.07
2SLS – Baseline, weather station data	-0.18	-0.34	-0.32	-0.16	-0.44**	-0.52**	-0.38
(C) Services							
2SLS - Baseline	-0.03	-0.19	-0.12	-0.32*	-0.20	-0.25	0.06
2SLS – Baseline – no Réunion	0.00	-0.19	-0.16	-0.22	-0.09	-0.28	-0.09
2SLS – Baseline, 3 lags shock	-0.03	-0.16	-0.10	-0.31*	-0.15	-0.22	0.12
2SLS –3 lags CPI	-0.08	-0.20	-0.17	-0.35**	-0.25	-0.30	0.01
2SLS – Baseline excl. shock < 6months	-0.04	-0.25	-0.16	-0.41*	-0.26	-0.33	0.07
2SLS – 6 lags forward	-0.18	-0.27	-0.30	-0.37**	-0.28	-0.27	-0.11
2SLS – Baseline, weather station data	-0.05	-0.15	-0.07	-0.19	-0.09	-0.17	0.24
(D) Energy							
2SLS - Baseline	-0.48	-0.20	0.35	-0.04	-0.25	-1.10	-1.17
2SLS – Baseline – no Réunion	-0.45	0.14	0.16	-0.33	-0.03	-0.74	-1.26
2SLS – Baseline, 3 lags shock	-0.46	-0.06	0.46	0.51	0.30	-0.71	-1.00
2SLS –3 lags CPI	-0.51	-0.30	0.20	-0.25	-0.44	-1.34*	-1.38*
2SLS – Baseline excl. shock < 6 months	-0.61	-0.25	0.44	-0.05	-0.34	-1.45	-1.57
2SLS – 6 lags forward	-0.81	-0.54	-0.04	-0.54	-0.65	-1.45*	-1.70**
2SLS – Baseline, weather station data	-0.48	-0.40	0.06	-0.44	-0.67	-1.56**	-1.97**
(E) Tobacco							
2SLS - Baseline	-0.04	-0.38	-0.35	0.00	-0.60	-0.32	-0.38
2SLS – Baseline – no Réunion	0.34	0.99	0.70	1.35	-0.06	0.22	-0.56
2SLS – Baseline, 3 lags shock	-0.37	-0.87	-0.15	0.43	0.43	0.58	0.47
2SLS –3 lags CPI	0.02	-0.51	-0.58	-0.19	-0.78	-0.60	-0.60
2SLS – Baseline excl. shock < 6 months	-0.10	-0.53	-0.45	0.00	-0.75	-0.49	-0.58
2SLS – 6 lags forward	0.50	0.77	0.90	1.00	1.22	1.46	1.53
2SLS – Baseline, weather station data	-1.03**	-1.56**	-1.07	-0.06	-0.92	-1.37	-1.78

***Note*:** The table shows alternative specifications of local projections of consumer prices. Panel (A) shows results for total CPI, panel (B) shows results for the CPI of fresh products. "2SLS baseline" is our baseline 2SLS specification. "2SLS – Baseline – no Réunion" is the baseline specification excluding Réunion. "2SLS – Baseline, 3 lags shock" controls for up to 3 lags of the shock (instrumented by relevant lags of the instrumental variables). "2SLS – 6 lags forward" controls for up to 6 forward lags of the shock. "2SLS – 3 lags CPI" controls for 3 lags of monthly variations of CPI. "Baseline excl. shock < 6 months" is the baseline specification, excluding shocks that occur less than 6 months after a previous shock. "2SLS – Baseline, weather station data" is the baseline specification, but with instruments taken from weather station data rather than remote sensing data.

*p < 0.10; **p < 0.05; *** p < 0.01.

Figure B.8. Baseline for fresh products CPI, including pre-trends up to 3 months

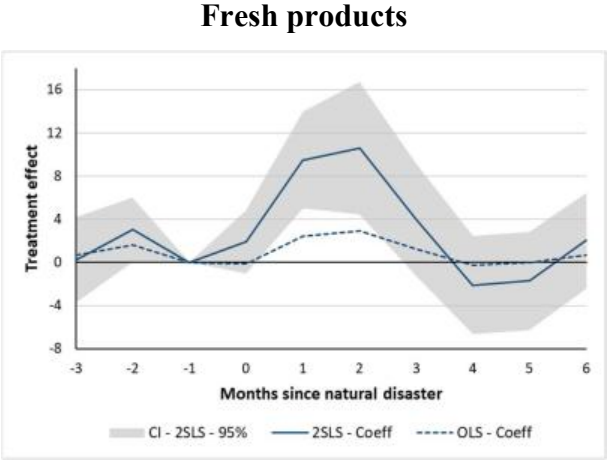

Note: The figure plots the cumulated impulse response function for the CPI of fresh products in our baseline IV specification (solid blue) and for the OLS specification (dotted blue). 95% confidence intervals for the 2SLS specification with robust standard errors in the shaded areas. Treatment effects are expressed in percent.

Appendix C. Constructing wind and rain damage functions

This section provides complementary information on the construction of damage functions. For the calibration of wind speed threshold value W^*, we follow Emanuel (2011) and set it to 50 knots. More specifically, we follow a two-step approach. Since remote sensing data is less precise for extreme values, we compute in a first step the percentile of wind speed above 50 knots from ground station recordings available through GSOD. In a second step, we apply the percentile to the remote sensing data from the CCMP in order to obtain a threshold value $\widehat{W}_i^*$ for each region and expressed in meters per second.

The calibration of region-specific rainfall threshold values r_i^* follows Heinen et al. (2018). The threshold is based on precipitation of 112 mm, cumulative over a three-day window, which Heinen et al. (2018) calibrated to an intensity duration flood model and actual flood event data for Trinidad. Given the heterogeneity of regions in our sample, with likely differing threshold values, we proceed in two steps. First, we compute the percentile of 112 mm over three-day windows for the closest region to Trinidad in our sample, i.e. Martinique. We then applied this percentile value to rainfall data of the remaining regions in our data sample to obtain regional threshold values in millimeters. The resulting threshold values are 229 mm for Réunion, 52 mm for Guadeloupe and 74 mm for French Guiana.

Exposure weights ξ_{ij} are constructed from satellite nighttime light data from the U.S. Air Force Defense Meteorological Satellite Program (DMSP), obtained via the Earth Observation Group (Baugh et al., 2010). We use the version cleaned of background noise, averaged across the calendar year and corrected for percent frequency of light detection. Figure C.1, panel a visualizes the data for the case of Réunion. Figure C.1 panel b shows nighttime light observations that are cleaned of observations above the ocean surface. We use geographic information system software and freely available shapefiles on ocean surfaces by *Natural Earth* to do so. The main motivation is to take into account noise from coastal areas, such as ships or other coastal activities. We compute a proxy of economic activity in a weather cell *j* in region *i* as

$$\nu_{ij} = \sum_{n=1}^{N} NTL_{ijn} \times \mathbb{1}_{\{O_{ijn}=0\}} \tag{C.1}$$

where NTL_{ijn} denotes nighttime light in region *i* in weather cell *j* and nighttime light grid cell *n*, and $\mathbb{1}$ denotes an index variable which takes the value of one if the nighttime light is recorded above land. Figure C.1 panel c illustrates that the number of nighttime light observations *N* per

weather cell *j* can vary substantially. The final weights are obtained by dividing nighttime light intensity in each weather cell *j* by total nighttime light intensity in region *i*:

$$\xi_{ij} = \frac{\nu_{ij}}{\sum_j \nu_{ij}} \tag{C.2}$$

Figure C.1 panel d illustrates the final result, while brighter areas indicate higher values of ξ_{ij}.

Figure C.1. Nighttime light weights for Réunion

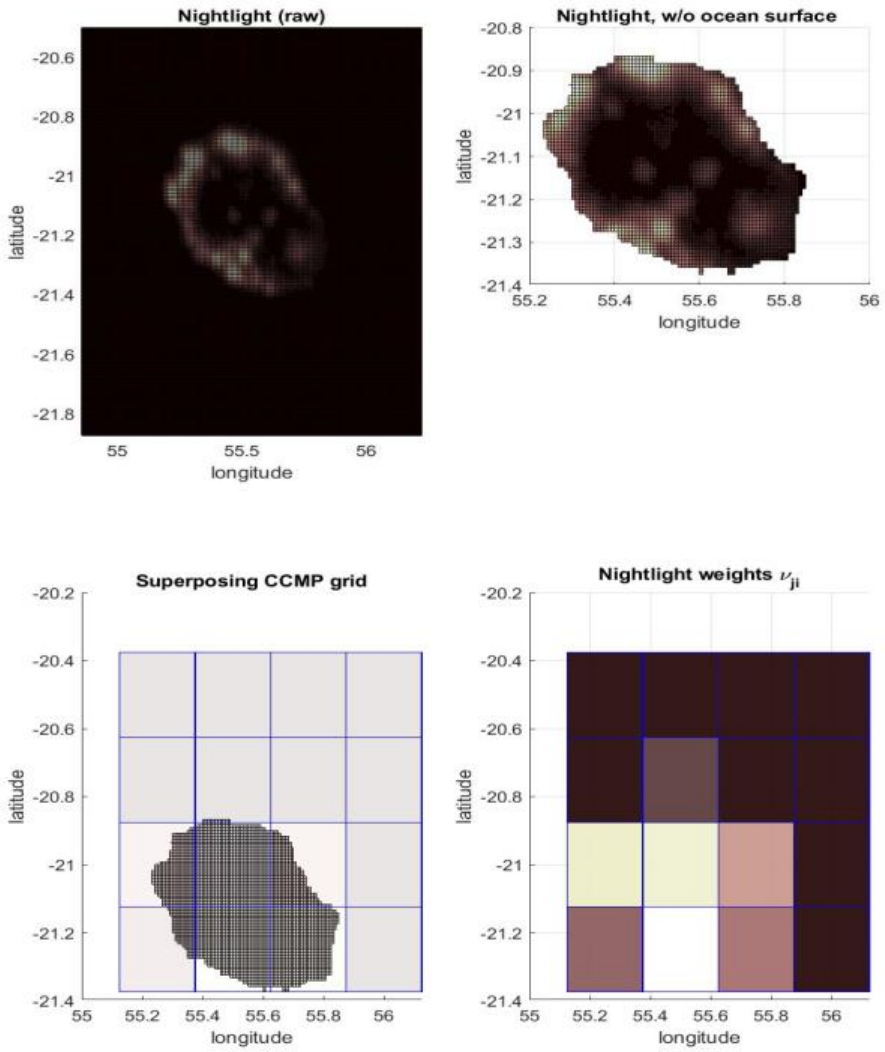

Note: Panel a: Satellite nighttime lights are from the Defense Meteorological Satellite Program (DMSP), average light for the calendar year 2000 times the percentage frequency of light detection. Panel b: Nighttime light w/o ocean surface makes use of the ocean surface shapefile from *Natural Earth.* Panel c: Weather cells are from the Cross-Calibrated Multi-Platform (CCMP). Panel d: Brighter cells of the final nightlight weights indicate higher share of total detected nighttime light, which is the proxy for regional economic activity.

Appendix D. Constructing an IRF for each quintile of income

The main difficulty in merging the CPI data with the *Budget des familles* is that the *Budget des familles* consumption basket and the CPI aggregates we considered, though based on the same underlying classification (COICOP), have differing compositions. This prevents perfect mapping of the two sets of items. We therefore focus on the item that reacts the most strongly in our estimation, namely food. However, reconciling the two data sets is not straightforward. Indeed, while INSEE publishes the CPI of fresh products and total CPI excluding fresh products, the share of fresh products in the consumption baskets is not available from the *Budget des familles* survey. Conversely, while the *Budget des familles* survey gives weight for total food (including tobacco), the food CPI published by INSEE excludes tobacco. We therefore resort to the following simple approximation. First, in the *Budget des familles* survey, for each quintile of income, and on average across the four overseas regions, we compute the percent deviation in the share of food (including tobacco), compared to the average share. Second, we apply these percent deviations to the average weight of fresh product observed in our sample. This gives us estimated weights of fresh products for each quintile. We therefore implicitly assume that the deviation of weights of fresh products between the quintiles and the average is the same as the observed deviation of weights of food including tobacco, and that the deviation of weights of food products observed in 2017 between the quintiles and the average is representative of the deviations that occurred between 1999 and 2018. Finally, we combine the estimated baseline impulse response functions for fresh products and total excluding fresh products with these set of weights for fresh products (and their respective counterparts, corresponding to the weights of total excluding fresh products for the different quintiles) to derive an estimated impulse response function of total CPI for each quintile.

Table D.1 – Share of food (including tobacco) in the household consumption basket, by quintile of income (2017)

	Guadeloupe	Martinique	French Guiana	Réunion	Average
Total	15.8	16.0	15.8	17.0	16.2
1st quintile	19.8	19.9	21.2	23.3	21.1
2nd quintile	20.1	18.0	20.7	21.9	20.2
3rd quintile	16.5	16.5	16.2	17.2	16.6
4th quintile	15.8	15.3	15.2	15.7	15.5
5th quintile	12.4	13.9	12.2	14.5	13.3

Note: This table presents the share of food (including tobacco) in the household consumption basket, according to the *Budget des Familles* survey of 2017. The average across the four DROMs is computed as an unweighted mean.

Appendix E. Deriving an optimal shock based on estimated shock probability using a ROC curve

We derive an optimal shock based on estimated shock probability using a ROC curve. To build the ROC curve, we discretize the range of observed values of predicted shock probability based on equation (1) (i.e. $\widehat{\omega}_{i,t,m}$) into 928 evenly spaced values, ranging from a minimum of -0.32 and a maximum of 1.18. For each value T among these 928 values, we define a discrete shock variable equal to one if $\widehat{\omega}_{i,t,m}$ is above T, and zero otherwise. For each of these discrete shocks, we compute a true positive rate (TPR, sensitivity) and a false positives rate (FPR, 1-specificity) using the following formulas:

$$TPR = \frac{True\ positive}{True\ positive + False\ negative}$$

$$FPR = \frac{False\ positive}{False\ positive + True\ negative}$$

True positive corresponds to the number of observations classified as a shock, which indeed are observed shocks; *false negative* is the number of observations not classified as a shock while there is actually a shock; *false positive is* the number of observations classified as a shock while there is actually no shock; *true negative* is the number of observations not classified as a shock when there is actually no shock.

The ROC curve in Figure E.1 plots TPR against FPR for all of the 928 discrete shocks defined above. The further the ROC line is from the diagonal line, the more successful is the model at identifying shocks.

We define the optimal threshold as the one that maximizes the following formula:

$$\sqrt{TPR \times (1 - FPR)}$$

The optimal threshold is 17.5%: we then define an observation as a shock when its underlying estimated probability of an administrative shock is higher than 17.5%. The confusion matrix of shocks derived under the optimal threshold is depicted in Table E.1. It shows that all actual administrative shocks are correctly classified as a shock, but that observations classified as a shock represent less than half of the total number of observations classified as a shock (69 out 177, 40%).

Figure E.1. ROC curve based on linear probability models with varying thresholds for shock discretization

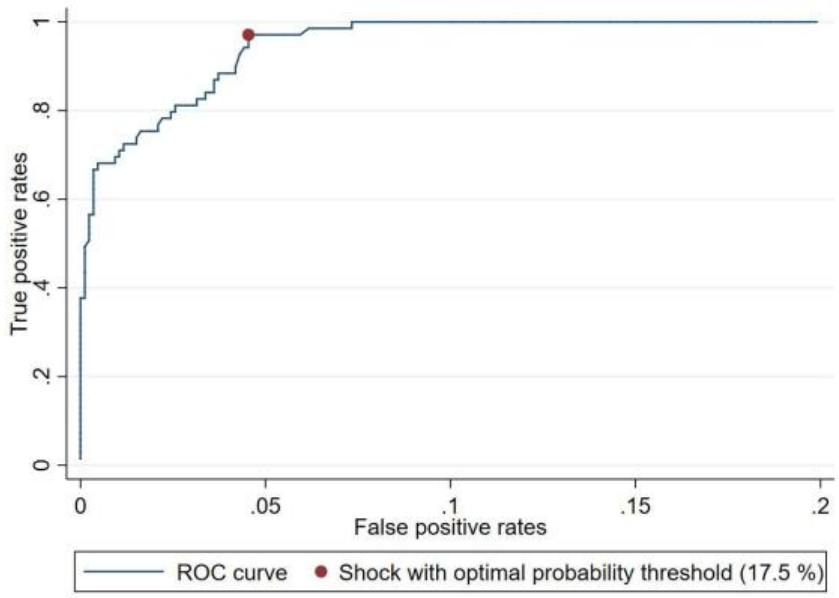

***Note*:** The curve represents the share of true positive shocks (i.e. the number of true positives divided by the sum of true positives and false negatives) against the share of false positives (i.e. the number of true positives divided by the sum of false positives and true negatives), for all of the 928 thresholds of predicted probability between 0 and 1. The red dot corresponds to the threshold maximizing the true positive rate while minimizing the false positive rate, and corresponds to a threshold of 17.5%.

Table E.1 – Confusion matrix for the optimal shock based on the ROC curve

	Pred. shock=0	**Pred. Shock=1**
True shock=0	751	108
True shock=1	0	69

Results from the regressions presented in Figure 9 are based on the following OLS specification for each of the 928 values of T:

$$\log\left(\frac{P_{i,t,m+h}}{P_{i,t,m-1}}\right) = \tau_h + \theta_h \mathbb{1}(\hat{\omega}_{i,t,m} > T) + \gamma_{i,h} + \delta_{t,h} + \theta_{m,h} + \theta_{m,h} \times R_{i,h} + \varepsilon_{i,t,m,h}$$

Figure E.2. Distribution of estimated effects on fresh products in the discrete shocks against the baseline effect

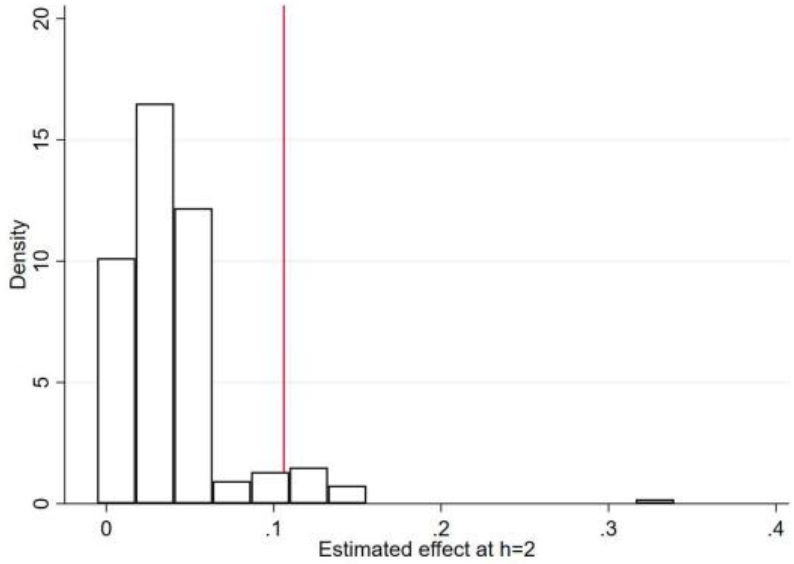

***Note**:* Distribution of estimated coefficients represented in Figure 9. The red line corresponds to the baseline 2SLS effect.

Appendix F. Drawing random weather shocks for placebo estimations

In this section, we describe how we draw random weather shocks for our first placebo estimation (in which we instrument the actual administrative shocks by randomly generating them). We model the maximum observed monthly rainfall and wind speed using Gumbel distributions. The latter are part of generalized extreme value distributions, which are well suited to modelling extreme phenomena such as the ones we focus on.

For wind and rain, we generate 100 random draws from Gumbel distributions whose parameters match the empirical moments of the maximum wind and rain distributions. More specifically, the expected value and variance of a random variable following a Gumbel distribution of location parameter μ and of scale parameter β are defined as:

$$E(X) = \mu + \beta\gamma$$

$$V(X) = \frac{\pi^2}{6}\beta^2$$

where γ is Euler-Mascheroni constant (approximated by the value 0.5772156649). We therefore define $\hat{\beta}$ and $\hat{\mu}$ as:

$$\hat{\beta} = \sqrt{6} \times \frac{\widehat{sd(X)}}{\pi}$$

$$\hat{\mu} = \widehat{E(X)} - \hat{\beta}\gamma$$

where $\widehat{sd(X)}$ and $\widehat{E(X)}$ are empirical standard deviation and expected values observed for the variable X in our full sample of observations. Empirically, $\hat{\beta}$ and $\hat{\mu}$ are similar to the parameters estimated in Stata using the package extremes. Using these sets of parameters, computed both for observed maximum records of wind speed and rainfall, we randomly generate placebo values of maximum records of wind speed and rainfall for these values, defining them as:

$$Max_{placebo} = \max(\hat{\mu} - \hat{\beta} \times \ln(-\ln(\mathrm{U})), 0)$$

where U is a random draw in a uniform distribution [0,1]. Since random draws in a Gumbel distribution can take negative values, we truncate them at zero, in order to match the fact that maximum rainfall and wind speed cannot have negative values.

In Figures F1 and F2, we plot the densities of placebo records (in grey), the density of observed records (in red), and the density of a random draw of a normal distribution with parameters of

expected value and standard deviation equal to the empirical moments of maximum wind speed and rainfall (in blue). In Figures F3 and F4, we plot the quantile-quantile (QQ) plots of our random draws against the observed distributions. Overall, our random draws match the distribution of observed maximum wind speed and rainfall reasonably well, and are better suited to such data than a normal distribution.

Table F.1 – Empirical moments of maximum wind and rainfall and computed parameters of Gumbel distributions

	$\widehat{E(X)}$	$\widehat{sd(X)}$	$\hat{\mu}$	$\hat{\beta}$
Maximum wind speed	11.49	2.07	10.56	1.61
Maximum rainfall	47.53	35.16	31.70	27.41

Figure F.1. Placebo and observed maximum wind speed

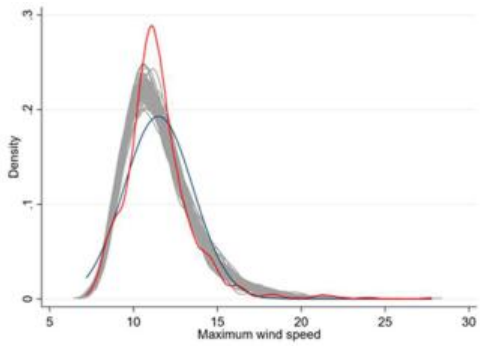

Figure F.2. Placebo and observed maximum rainfall

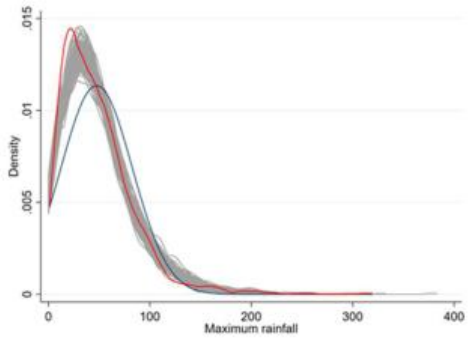

***Note*:** The grey curves represent 100 densities of random draws in Gumbel distributions matching the observed moments of maximum wind speed and maximum rainfall. Blue curves correspond to a random draw in a normal distribution. Densities of actual maximum wind speed and rainfall are plotted in red.

Figure F.3. QQ plots of placebo and observed maximum wind speed

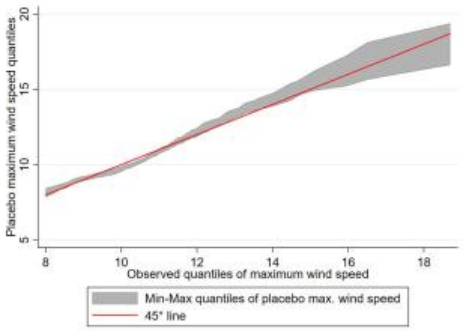

Figure F.4. QQ plots of placebo and observed maximum rainfall

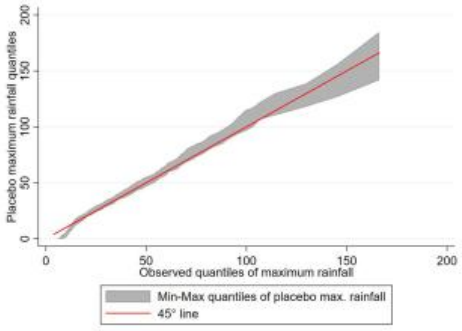

***Note*:** The figures plot the range of quantiles of placebo maximum wind speed (resp. placebo maximum rainfall) against the respective quantiles of observed maximum wind speed (resp. observed maximum wind speed).